UNITED STATES DEPARTMENT OF THE INTERIOR

GEOLOGICAL SURVEY

INTERPRETATIONS OF MAGNETIC ANOMALIES AT A POTENTIAL REPOSITORY SITE
LOCATED IN THE YUCCA MOUNTAIN AREA, NEVADA TEST SITE

By

G. D. Bath and C. E. Jahren

Open-File Report 84-120

Prepared in cooperation with the
Nevada Operations Office
U.S. Department of Energy
(Interagency Agreement DE-AI08-78ET44802)

Denver, Colorado
1984

CONTENTS

i

ILLUSTRATIONS

TABLE

UNITED STATES
DEPARTMENT OF THE INTERIOR
GEOLOGICAL SURVEY

INTERPRETATIONS OF MAGNETIC ANOMALIES AT A POTENTIAL REPOSITORY SITE LOCATED IN THE YUCCA MOUNTAIN AREA, NEVADA TEST SITE

By

G. D. Bath and C. E. Jahren

ABSTRACT

In the Yucca Mountain area near the southwestern border of the Nevada Test Site, studies of the relation of magnetic properties to geologic features have provided structural information at and near a potential site for storage of radioactive waste. Interpreted features include a tabular mass of magnetized sedimentary rock beneath thick deposits of volcanic rock, and 11 major faults that strike generally northward and displace magnetized volcanic rock. A positive anomaly in a high-altitude aeromagnetic survey over exposures of strongly magnetized argillite of the Eleana Formation extends westward 20 km into the site area where interpretations indicate an argillite thickness of 800 m at a depth of 2.25 km. The high magnetite content of the argillite is not typical of the region, and was probably introduced by the heating effects of an underlying pluton. The basis for mapping traces of faults, and identifying their upthrown sides, was developed elsewhere at Yucca fault in the relatively simple volcanic terrains of Yucca Flat. In the site area, analyses of aeromagnetic anomalies from a low-altitude east-west aeromagnetic survey show the Topopah Spring Member of the Paintbrush Tuff as the primary source of anomalies from faulted sequences of volcanic rock. Faults related to belts of positive and negative anomalies surrounding the site have been identified. The possibility that an east-west pattern of anomalies is related to structure crossing the site was investigated by a recent aeromagnetic survey flown at low altitude in north-south directions. A significant reduction in amplitude of these anomalies resulted when effects of the deeply buried argillite were removed. The remaining anomalies over the site can be explained by a change in lateral extent, or magnetic properties, of volcanic units beneath the Topopah Spring Member.

INTRODUCTION

Air and ground magnetic surveys were undertaken in the southwestern region of the Nevada Test Site (NTS) to investigate the relation of magnetic anomalies to buried geologic features at the Yucca Mountain site, which is being evaluated as a potential repository for storage of high-level radioactive waste. This study is similar to several the USGS has made at NTS and nearby areas to locate large bodies of buried magnetic rock, and to estimate their depths and shapes. This work was performed for the Nevada Nuclear Waste Storage Investigations (NNWSI) project of the U.S. Department of Energy (DOE).

1

Yucca Mountain is underlain by a thick sequence of ash-flow tuffs and tuffaceous sediments, and subordinate amounts of lava flow and flow breccia. The volcanic rocks are of Tertiary age and attain a combined thickness of more than 1,829 m (6,000 ft). Pre-Tertiary rocks consist of older sedimentary rock with the possibility of igneous intrusions. Well-defined individual anomalies in an aeromagnetic survey 2,450 m (8,000 ft) above sea level trend east-west, and are interpreted as arising from a deep source of older sedimentary rock having an increased magnetite content from the heating effects of an underlying pluton. More complex anomaly patterns in an aeromagnetic survey 120 m (400 ft) above the surface are alined generally north-south, and are interpreted as arising from edges of volcanic flows that have been formed by vertical displacements along major faults. A prominent east-west pattern of anomalies crossing the site area is interpreted as the effect of the deep source superimposed on numerous effects of near-surface volcanic rock. Kane and Bracken (1983) report the patterns include prominent anomaly trends that are typically elongate to the north or northeast.

Standard methods of interpretation were used, and their application to a major fault structure was illustrated in detail at the Yucca fault in the relatively simple volcanic terrains of Yucca Flat. Average magnetic properties of geologic units were estimated from extensive measurements of surface and drill-core samples, from interpretations of downhole magnetometer logs, and from interpretations of short wavelength anomalies found in ground magnetic surveys. In order to isolate anomalies for modeling studies, we have defined a magnetic reference surface having zero magnetic anomaly over large areas of thick, nonmagnetic, sedimentary rock. Our reference surface is located in the Mercury area, and long truck-borne magnetometer traverses (fig. 1) were used to carry the reference value into the Yucca Mountain and Calico Hills areas.

Figure 1 shows the large bodies that produce anomaly amplitudes greater than 200 nT (200 gammas) at the 2,450-m (8,000-ft) elevation in the NTS region. Several bodies are normally magnetized in the approximate direction of the Earth's magnetic field and produce anomaly maxima. Normally magnetized intrusive bodies include the Climax and Gold Meadows stocks in the northeast part of NTS at the 462 and 329 nT maxima near A (fig. 1) in the northwest corner of NTS, at the 316 and 312 nT maxima at B; near Black Mountain at the 548 and 525 nT maxima at C; and near the southeast corner of NTS at Wahmonie Flat at the 312 nT maximum near D. The broad positive anomaly having maxima of 547 and 388 nT northwest of D arises from strongly magnetized sedimentary rock that is exposed at Calico Hills and extends at depth toward Yucca Mountain. The 219 nT maximum in the Yucca Mountain area is interpreted as the consolidated effects of near-surface volcanic rock, and buried sedimentary
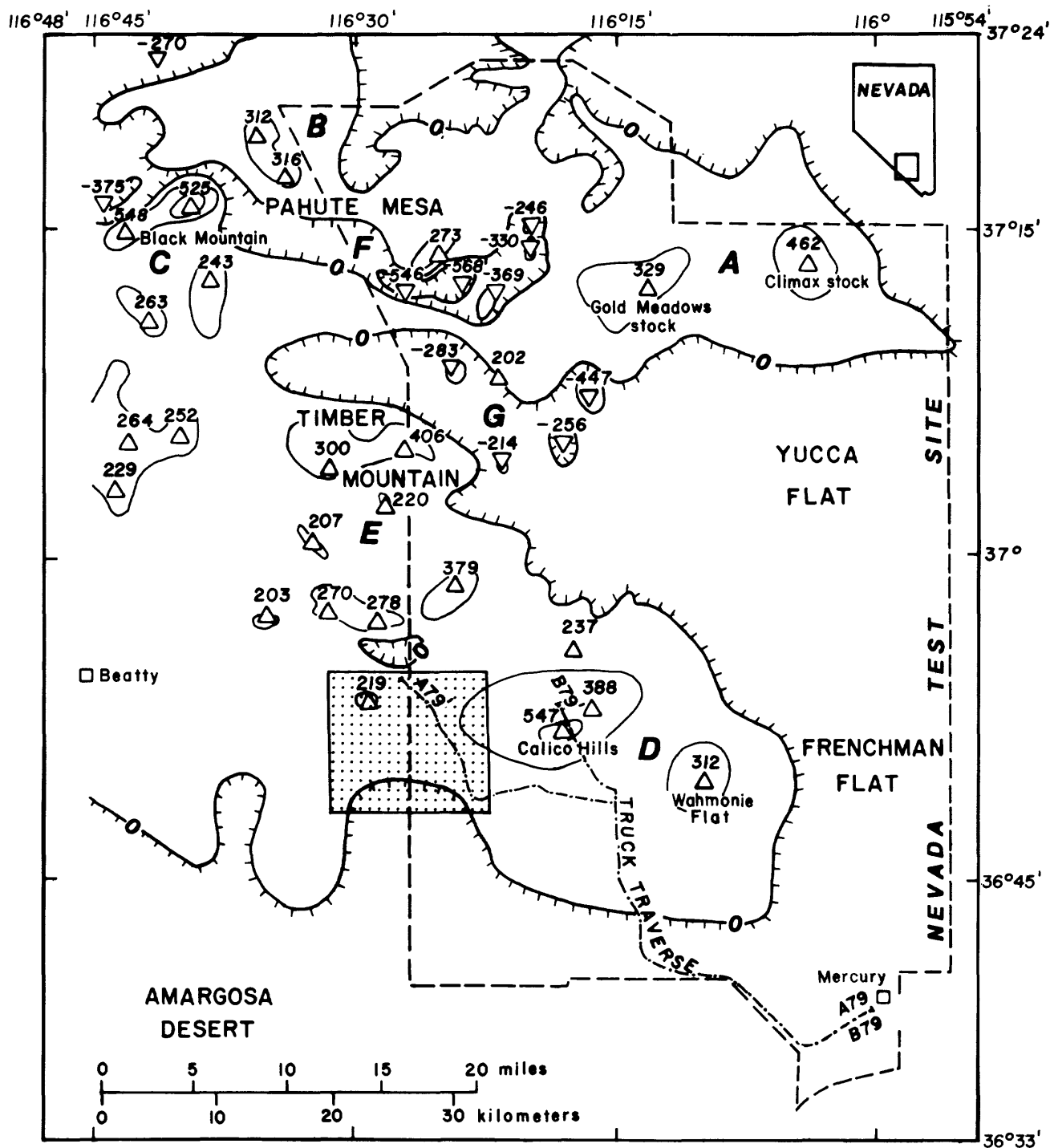
Figure 1.--Residual aeromagnetic map of Nevada Test Site and nearby areas showing the Yucca Mountain area (shaded), areas of outstanding anomaly maxima by letters A through E, and areas of outstanding anomaly minima by letters F and G. Also shown are truck-borne magnetometer traverses A79-A79' and B79-B79' from Mercury to the Yuccca Mountain and Calico Hills areas.

3

rock that has been metamorphosed by an underlying intrusive. A combination of normally magnetized volcanic rock and buried intrusive was interpreted by Kane and others (1981) as the probable source of the 406 and 300 nT maxima at Timber Mountain north of E. Magnetic property measurements also denote reversely magnetized rock that produce prominent negative anomalies. The anomalies east of F that have minima of -546, -568, -369, -330, and -246 nT on the southern flank of Pahute Mesa are caused by reversely-magnetized rhyolite flows (Bath, 1968). Similarly, the minima of -283, -214, -256, and -447 nT near G and northeast of Timber Mountain, are caused by reversely-magnetized rhyolite and ash flows.

The residual anomalies shown on figure 1 were compiled by subtracting a regional field from the observed anomalies, a process designed to give values near zero over our standard reference surface near Mercury in the southeastern corner of NTS. A planar regional field was determined approximately by applying a least-square procedure to data, at 3-km (1.86-mi) grid intervals for the very large area of 10,000 km^2 (3,860 mi^2) covered by 14 published aeromagnetic maps including NTS and most of the Nellis Air Force Bombing and Gunnery Range (Boynton and Vargo, 1963a,b; Boynton and others, 1963a,b; and Philbin and White, 1965a-j). The regional field increeases 5.63 nT/km northward and 1.72 nT/km eastward. A graphical method was used to remove regional from observed contours.

System Of Magnetic Units

In this paper all magnetic units are given in the International System of units (SI). Conversions to the older electromagnetic units (emu) are given in the following table:

Quantity	SI unit	Equivalent unit (in emu)
Magnetic field	nanotesla (nT)	1 nT = 1 gamma
Magnetization	ampere/meter (A/m)	1 A/m = 10^{-3} gauss[1]

[1] The gauss, originally a cgs unit, is often used informally as 10^{-4} tesla in the SI system.

Acknowledgments

Several geologists and geophysicists have contributed to this report and their assistance is gratefully acknowledged. In particular, thanks go to W. J. Carr for discussing relations of anomalies to geology of Yucca Mountain, G. L. Dixon for discussing relations of anomalies to geology of Yucca Flat, and D. L. Shiel for measuring ground magnetic traverses. J. G. Rosenbaum provided most of the magnetic property data and wrote the three-dimensional forward program that sums individual magnetic anomalies calculated for a set of right polygonal prisms.

4

DEEP SOURCE AT YUCCA MOUNTAIN

The positive anomaly of long wavelength surveyed at high altitude over Yucca Mountain (fig. 2) can be explained by a deep source underlying volcanic rock in the northern half of the area. The anomaly is the westward continuation of the 547 nT maximum (near D of figure 1) from Calico Hills extending 20 km (12.4 mi) into the Yucca Mountain area. A simple two-dimensional model of the source was derived from an inverse analysis of anomalies along two long traverses, which provided constraints on depth and thickness. The assumption of continuation from Calico Hills provided magnetization values and geologic setting. The model is similar to the one at Calico Hills: a tabular body of sedimentary rocks containing magnetite, probably introduced by the heating effects of an underlying pluton. The inversion procedure, herein referred to as the KPQ method, is based on well-documented publications by Koulomzine and others (1970), Powell (1967), and Qureshi and Nalaye (1978).

High-Altitude Survey

The residual aeromagnetic survey shown on figure 1 was recompiled with contours at 20 rather than 200-nT intervals (fig. 2). The survey was along east-west traverses about 0.8 km (0.5 mi) apart and at a constant elevation of 2,450 m (8,000 ft). The Calico Hills positive anomaly extends westward from A to the maxima at B and C. Contours along the south slope, which includes the area of the proposed site, are generally parallel to the trend of the anomaly maxima.
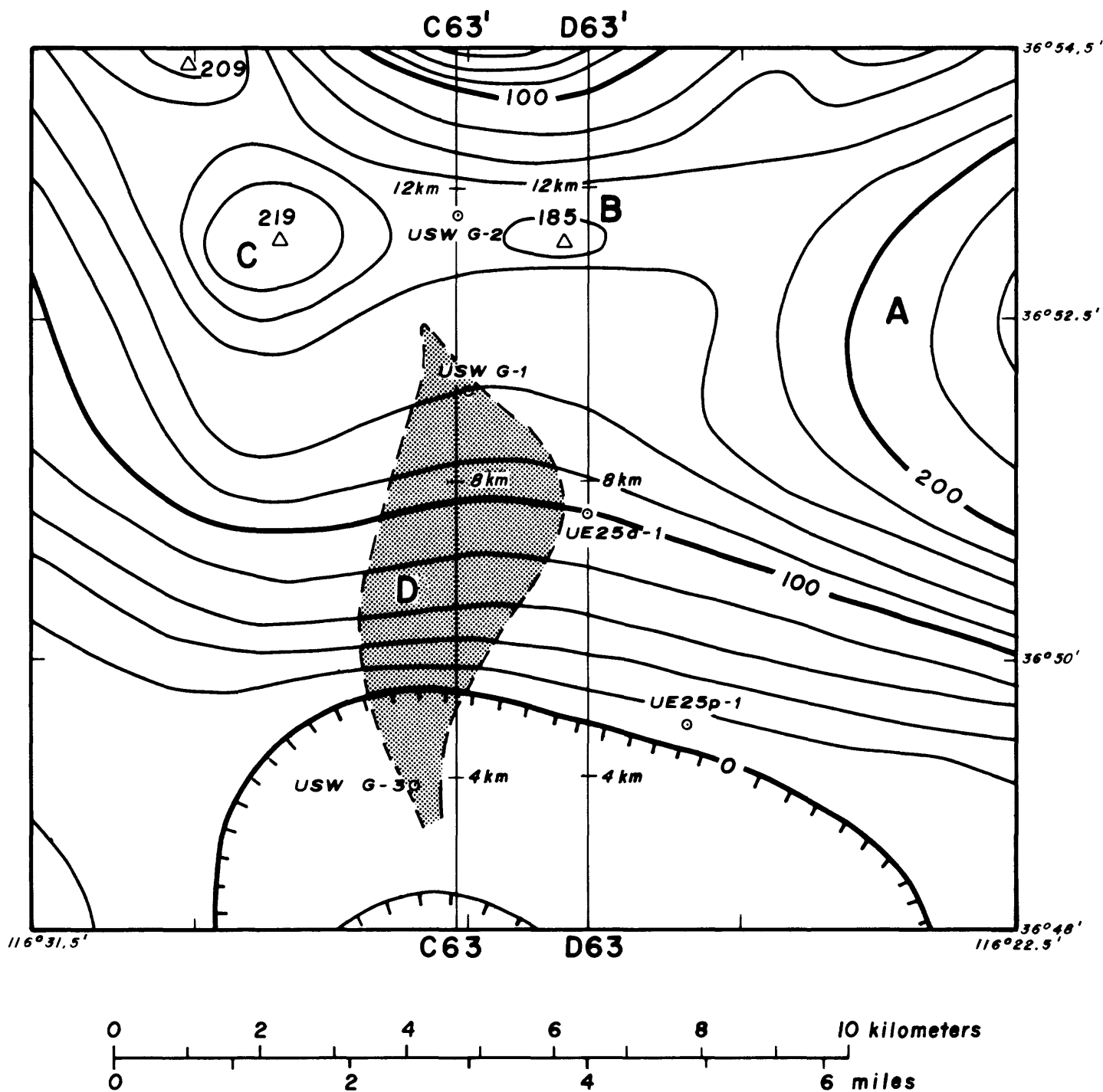
Figure 2.--Residual aeromagnetic map of Yucca Mountain area showing broad
positive anomaly extending westward from A to maxima of 185 nT at B and
219 nT at C. Also shown are current (1983) proposed site area (shaded),
parts of traverses C63-C63' and D63-D63', five drill holes, and the small
change in spacing of contours over the site at D.

Magnetic Properties

Air and ground magnetic surveys will commonly detect a geologic unit when its average total magnetization is equal to or greater than 0.05 A/m (10^{-3} emu). Therefore, units having intensities less than 0.05 A/m are herein designated nonmagnetic; and those having greater intensities are herein arbitrarily designated as either weakly, moderately, or strongly magnetized, as defined by the following limits:

$$\text{nonmagnetic} < 0.05 \text{ A/m}$$
$$0.05 \text{ A/m} < \text{weakly magnetized} < 0.50 \text{ A/m}$$
$$0.50 \text{ A/m} < \text{moderately magnetized} < 1.50 \text{ A/m}$$
$$1.50 \text{ A/m} < \text{strongly magnetized}$$

The average total magnetization of a uniformly magnetized rock mass, denoted as the vector $\vec{J}_t$, is defined as the vector sum of the induced magnetization, $\vec{J}_i$, and remanent magnetization, $\vec{J}_r$:

$$\vec{J}_t = \vec{J}_i + \vec{J}_r.$$

Methods used at NTS for measuring induced and remanent magnetizations of surface and drill-core samples, and for estimating total magnetizations from downhole magnetometer logs and ground magnetic surveys are given in data presented in Bath and others (1983).

Estimates of total magnetization of near-surface rocks vary from nonmagnetic to strongly magnetized along roads in the southern and southwestern parts of NTS. Magnetizations are based on the amplitudes of residual anomalies measured along two traverses (fig. 3) originating at Mercury. Traverse A79-A79' extends for 60.5 km (37.6 mi) to Yucca Wash, just north of the proposed site and over the deep source; and traverse B79-B79' extends 46.8 km (29 mi) to Calico Hills, and over outcrops of the argillite that is interpreted as the deep source at the repository site. Residual anomalies of short wavelength (A of fig. 3) indicate the pre-Tertiary sedimentary rocks from Mercury to Rock Valley and the alluvium along both traverses as nonmagnetic, and most volcanic rock as weakly to moderately magnetized. Examples of strongly magnetized rock are the Basalt of Skull Mountain at Little Skull Mountain, and the metamorphosed argillite at Calico Hills. Continued anomalies of long wavelength (B of fig. 3) indicate large volumes of magnetized rock that include buried pre-Tertiary rocks between Mercury and Rock Valley; volcanic rocks at Little Skull Mountain, buried along Jackass Flats, and at the surface and buried along Yucca Wash; and metamorphosed argillite at the surface at Calico Hills and buried at Yucca Wash.

Baldwin and Jahren (1982) have reported results of extensive studies of magnetic properties at Calico Hills. Strongly magnetized argillite of the Eleana Formation (Mississippian-Devonian age) is the principal cause of prominent air and ground magnetic anomalies. This property differs markedly from that characteristic of older sedimentary rocks elsewhere on NTS. Deposits of these rocks are usually thick, nonmagnetic, and present in areas of relatively uniform magnetic field. At Calico Hills, nonmagnetic argillite has been altered to magnetized rock, apparently by heating effects, which have converted pyrite to magnetite (Bath and others, 1983). The argillite is normally magnetized, and 123 samples of drill core varied in intensity from nonmagnetic to 26.6 A/m. Total magnetization averages 3.89 A/m for samples collected from two intervals having a total thickness of 365.5 m (1,200 ft). The value is the largest found for a magnetized geologic feature in the NTS region.
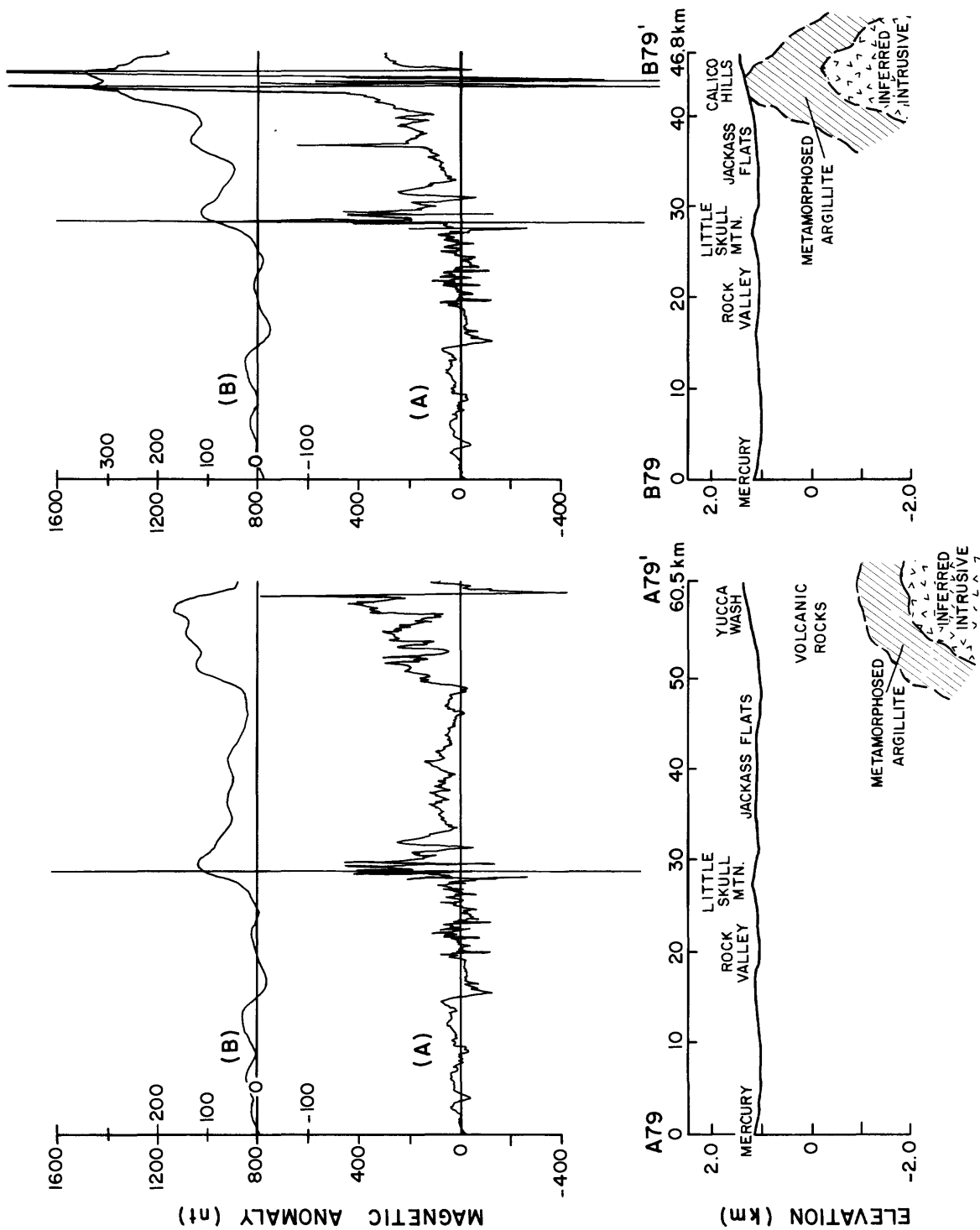
Figure 3.--Magnetic anomalies plotted at 48-m (157-ft) intervals along traverse A79-A79' from Mercury to Yucca Wash, and traverse B79-B79' from Mercury to Calico Hills. Anomalies (A) were measured with a truck-borne fluxgate magnetometer 4 m (13 ft) above the road surface and converted to residual values. Anomalies (B) are anomalies (A) after continuation upward 1,130 m (3,700 ft) to air datum of figures 1 and 2 by method of Henderson and Zietz (1949). The above figure includes road elevations, landmarks, and a cartoon showing metamorphosed argillite and inferred intrusive.

9

Anomaly Analysis

Almost all of the broad positive anomaly is assigned to effects of a deep
source. The irregular patterns of positive and negative anomalies outlined in
low-altitude surveys arise from a thick sequence of volcanic rock, but the
anomalies tend to merge and cancel in surveys at high altitude. Exceptions
are local anomalies from a few strongly magnetized units: the high of 185 nT
near B, the high of 219 nT near C, and others. The cancellation is
illustrated on figures 1 and 2 by values near zero over a typical sequence of
volcanic rock along the southern part of the site. Also, the zero contours
designate as nonmagnetic the thick pile of older sedimentary rocks beneath the
volcanic rocks.

The KPQ inverse method indicates the large positive anomaly can be
explained by a sheetlike source with its center at an elevation of -1,280 m
(-4,200 ft) below sea level. The analysis was from data obtained along two
long north-south profiles, C63-C63' and D63-D63', and shown as profiles on
figures 4 and 5. The source extends in both the east-west strike direction
and the north-south dip direction. It is designated sheetlike because the
thickness is less than one-half the depth of 3.73 km (2.32 mi) beneath the air
datum. The thickness is, therefore, too "thin" to be evaluated by this
method.

The tabular model shown in section on figures 4 and 5 was determined by
progressive modification of assumed models until a reasonable fit was found
for anomalies observed, and anomalies calculated with a three-dimensional
forward program. The source rock consists of magnetized Eleana Formation, and
represents a westward extension of the rocks at Calico Hills. The
magnetization is, therefore, normal with a total intensity of 3.89 A/m. The
model is a rectangular vertical prism with its horizontal top at an elevation
of -885 m (-2,900 ft). The prism is 14 km (8.7 mi) long east-west, 7.6 km
(4.7 mi) wide north-south, and 825 m (2,700 ft) thick.

10
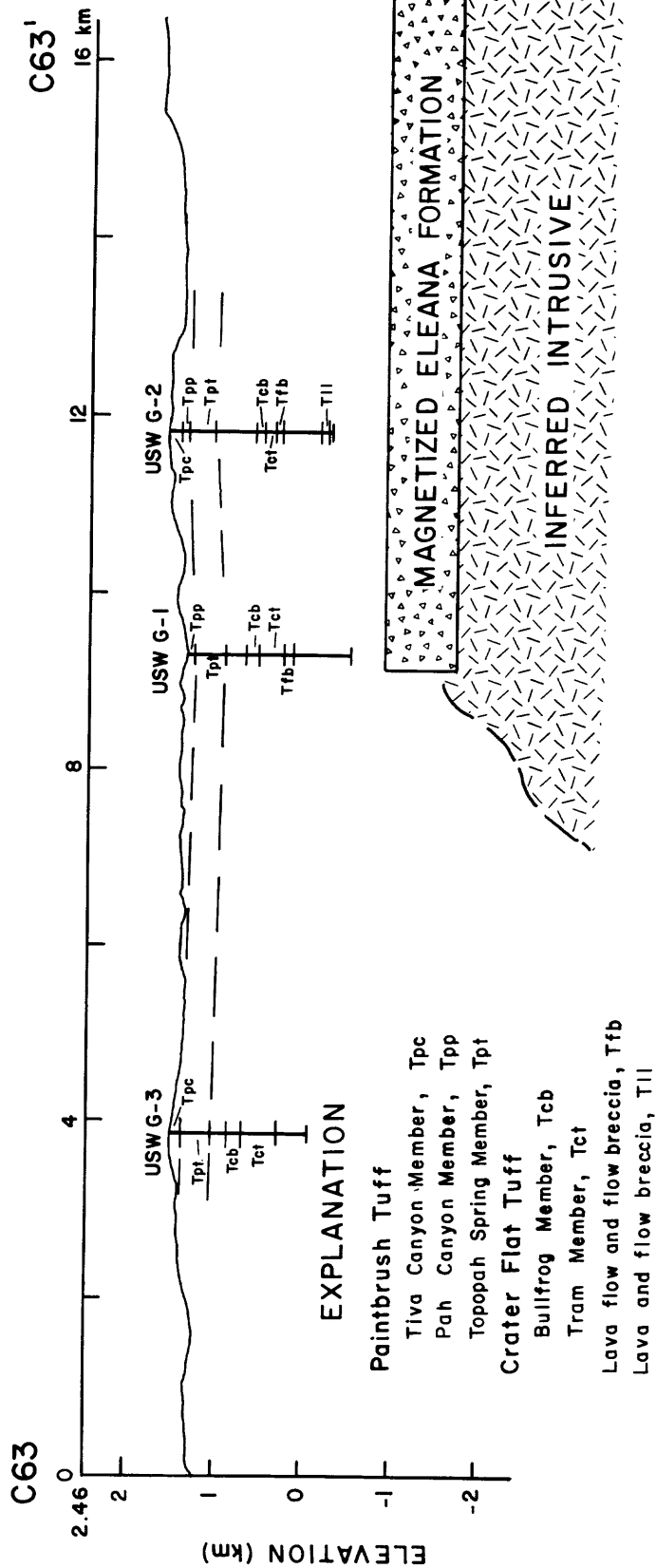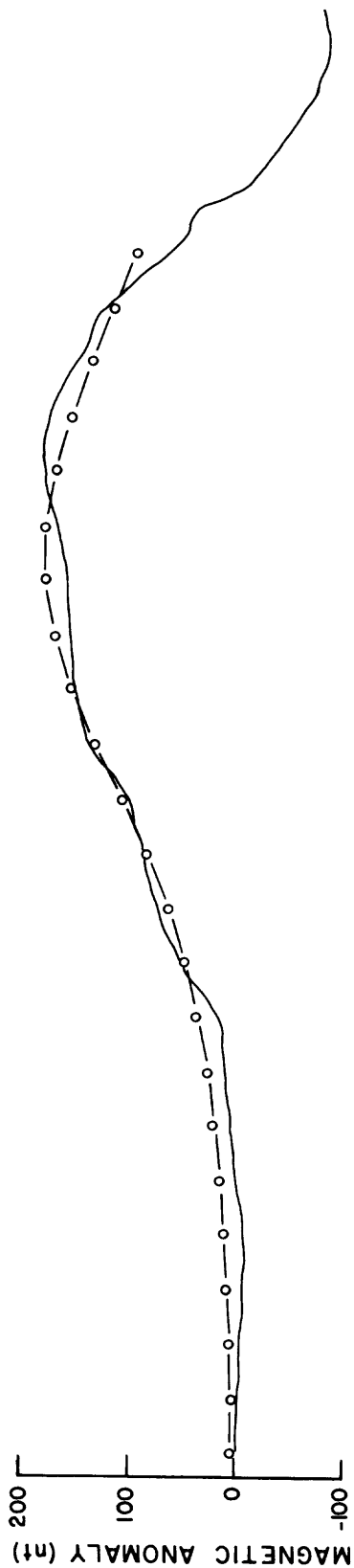
Figure 4.--Cross section along traverse C63-C63'' and through the model of strongly magnetized Eleana Formation. Residual anomaly is solid line, and anomaly of model is line with values computed at circles. Also shown are the magnetized Tertiary volcanic units that were penetrated in drill holes USW G-3, USW G-1, and USW G-2.

11

Figure 5.--Cross section along traverse D63-D63' and through the model of strongly magnetized Eleana Formation. Residual anomaly is solid line, and anomaly of model is line with values computed at circles. Also shown are the magnetized Tertiary volcanic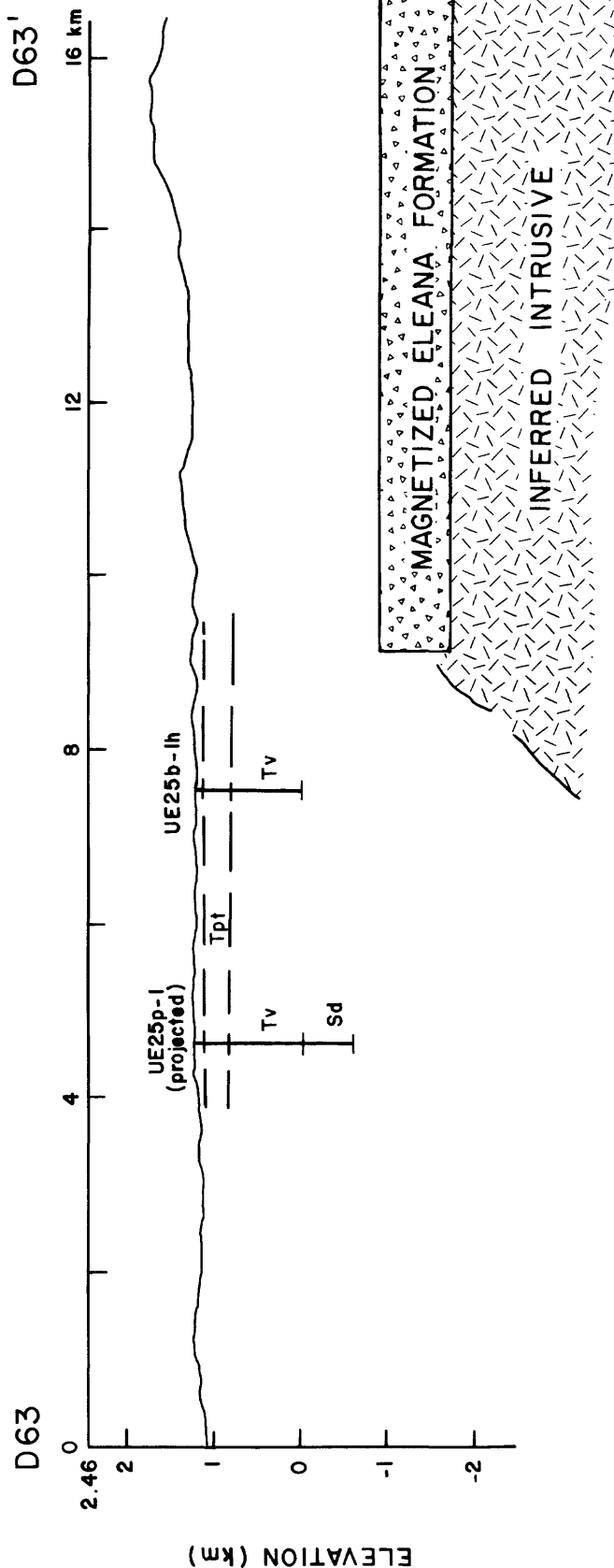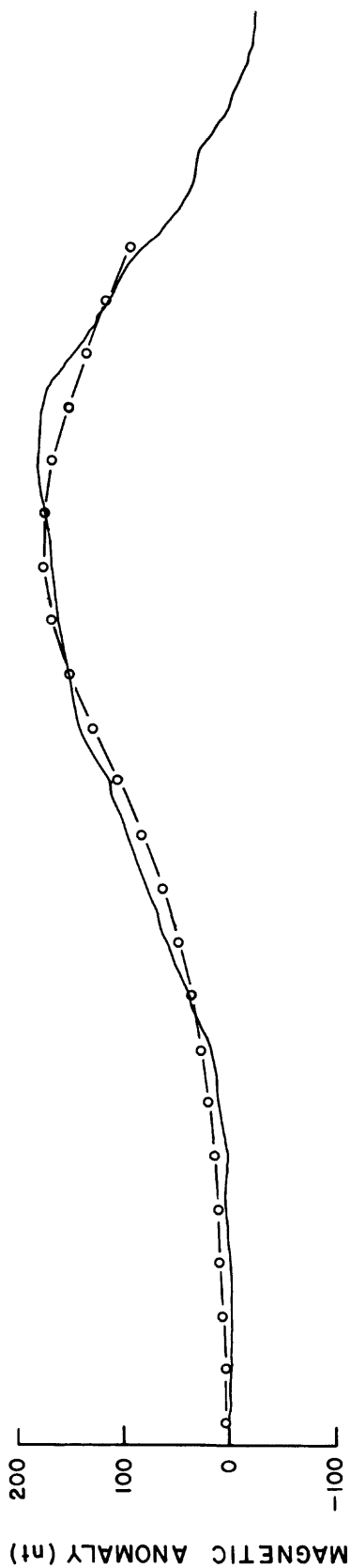 units (Tpt and Tv) penetrated in drill hole UE25b-1h, and the magnetized Tertiary volcanic units (Tpt and Tv) and nonmagnetic Silurian dolomite (Sd) penetrated in drill hole UE25p-1.

12

The interpretations infer strongly magnetized Eleana Formation and weakly magnetized intrusive rock beneath the northern part of the site as shown on figures 3, 4, and 5. The Eleana Formation (Gordon and Poole, 1968) is 380 m (1,250 ft) below the 1,829 m (6,000 ft) of Tertiary volcanic rock penetrated in drill hole USW G-1 (Spengler and others, 1981) and 610 m (2,000 ft) below the 1,829 m (6,000 ft) of Tertiary volcanic rock penetrated in drill hole USW G-2 (Maldonado and Koether, 1983) (fig. 4). Nonmagnetic dolomite of Silurian age was found at an elevation of -76m (-250 ft) in drill hole UE25p-1 (M. D. Carr, written commun., 1983) located about 2.68 km (1.7 mi) south of the inferred Eleana Formation (fig. 5).

The anomaly is explained entirely by Eleana Formation, and the magnetic effect of an underlying intrusive was not included in the analysis. This is consistent with preliminary analyses of magnetic anomalies at Calico Hills, and with the relatively low values of magnetization for nearby intrusives. Bath and others (1983) report magnetizations of intrusive rocks in drill holes at the Climax stock vary from 0.13 A/m at the surface to 1.2 A/m at a depth of 530 m (1,740 ft). These values are low in comparison with the 3.89 A/m average reported by Baldwin and Jahren (1982) for magnetized Eleana Formation.

RELATION OF ANOMALIES TO YUCCA FAULT AT YUCCA FLAT

Aeromagnetic surveys in the Yucca Mountain area, and in Yucca Flat in the northeastern part of NTS, were flown only 120 m (400 ft) above the surface, and close enough to detect anomalies produced by magnetized volcanic rock displaced by major faults (Bath and others, 1982; and Bath, 1976). The methods used to study fault anomalies were developed at the Yucca fault in Yucca Flat where only two anomaly-producing units are present in the subsurface. Included are qualitative methods using simple ratios and quantitative methods using models. The investigations have provided a basis for mapping the fault trace, identifying the upthrown side of the fault, and examining effects of increasing the vertical displacement of the fault.

In Yucca Flat, a single pair of parallel anomalies of positive and negative sense (fig. 6) can be explained by the edge effects of a single ash flow terminated by vertical displacement at the Yucca fault. The anomalies trend north-south for more than 17 km (10.6 mi) in Yucca Flat where volcanic tuffs buried by alluvium dip at low angles to the southwest. Magnetic properties of the flows are known from measurements of drill core and surface samples, and from interpretations of downhole magnetometer logs. The negative anomalies are over the upthrown side of the fault, and the positive anomalies are over the downthrown side. Inverse analysis indicates both air and ground anomalies can be explained by a thin dike or sheet that varies in depth from 70 m (230 ft) to 200 m (655 ft), and has a reversed direction of magnetization. Geologic studies (Dixon and others, 1975) show the Rainier Mesa Member of the Timber Mountain Tuff (Tmr) is present at these depths. This ash flow has a wide extent over much of Yucca Flat, and magnetic property measurements show it is reversely magnetized.
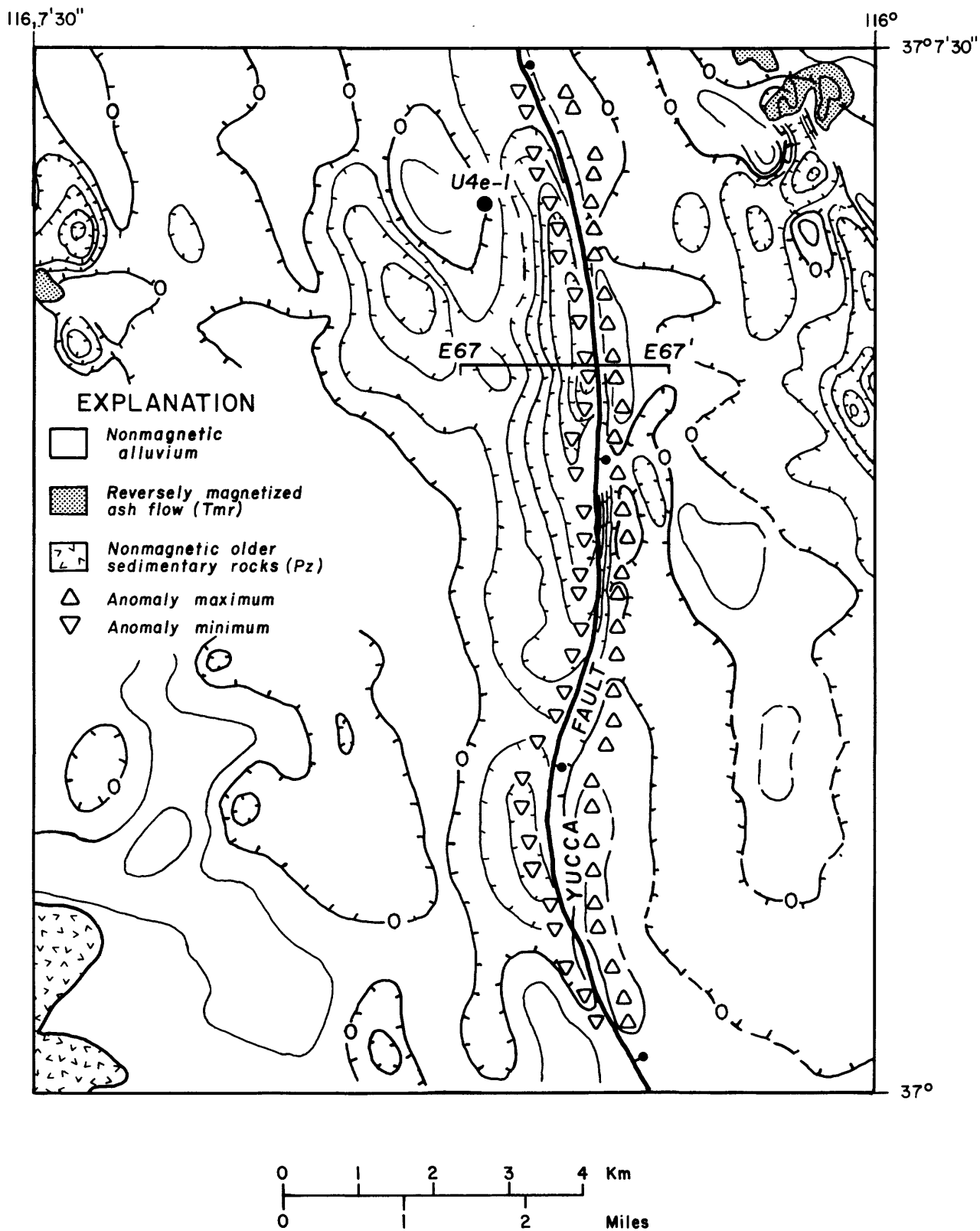
13

Figure 6.--Residual aeromagnetic and geologic map of the Yucca Flat quadrangle
showing positions of maxima and minima along Yucca fault, ground magnetic
traverse E67-E67', and drill hole U4e-1. Aeromagnetic data measured
along east-west traverses 120 m (400 ft) above the surface; contour
interval = 20 nT.

Low-Altitude Survey

The aeromagnetic survey of Yucca Flat (Bath, 1976) was along east-west traverses about 400 m (1,300 ft) apart and 120 m (400 ft) above the surface. The residual anomalies of figure 6 were compiled by removing effects of a regional anomaly and numerous drill-hole casings from the observed anomalies. The regional anomaly was developed by using a least-square process to adjust observed values at 1-km (0.62-mi) grid intervals to a sixth-order surface for an area of 700 km^2 (16.5 mi^2) in Yucca and Frenchman Flats. Short wavelength anomalies located directly over known strings of casing were removed from the original flight-line data.

Magnetic Properties

Yucca Flat is one of several alluvium-filled basins in the NTS region characterized by thick Tertiary volcanic rocks overlying very thick Paleozoic and uppermost Precambrian sedimentary rocks. Magnetic properties of surface and drill-core samples reported by Bath (1968 and 1976) designate volcanic flows as moderate to strongly magnetized, and alluvium and older sedimentary rocks as nonmagnetic.

In the magnetometer and generalized geologic logs of drill hole U4e-1 shown on figure 7, prominent anomalies correlate with positions of two ash flows on the upthrown side of the Yucca fault. Anomalies are positive within reversely magnetized units, and negative within normally magnetized units (Douglas and Millett, 1978; and Bath, 1976). There is a negative anomaly for an interval of 43 m (142 ft) within the Ammonia Tanks Member of the Timber Mountain Tuff (Tma), and a positive anomaly for an interval of 127 m (415 ft) within the Rainier Mesa Member of the Timber Mountain Tuff (Tmr). Irregular anomalies of short wavelength correlate with intervals of nonmagnetic rock: 340 m (1,115 ft) of alluvium; 440 m (1,445 ft) of air-fall, bedded, zeolitized, and reworked tuff; and 25 m (82 ft) of sedimentary rocks of Paleozoic age. The downhole magnetometer passes very close to the rock, and observed anomalies are large, varying from -1,400 to 6,800 nT.
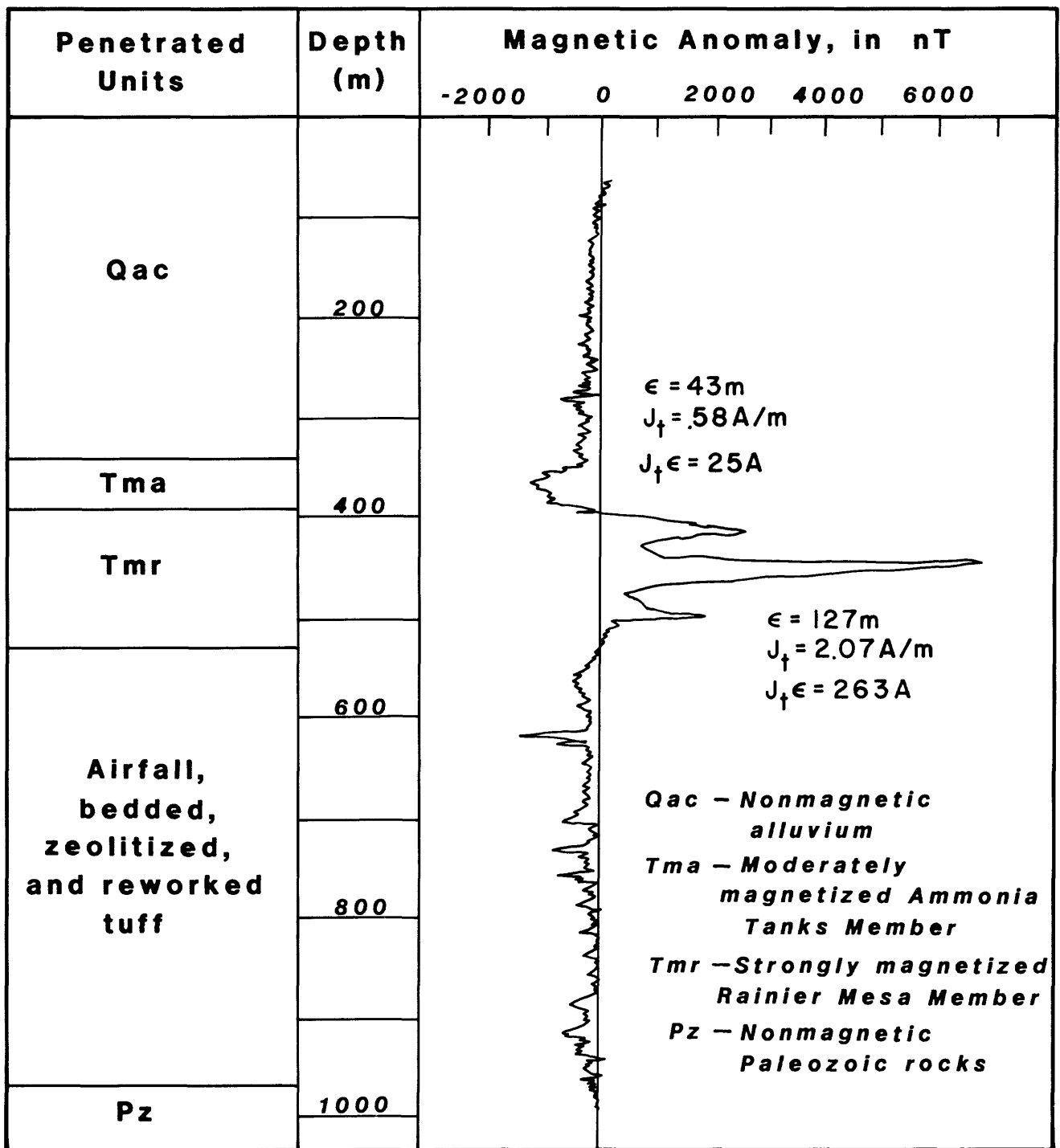
15

Figure 7.--Proton magnetometer and general geologic logs of drill hole U4e-1. Thickness of magnetic facies, ε, total magnetization, J_t, and product $J_t\varepsilon$ are given for negative anomaly at Tma and positive anomaly at Tmr.

16

The products of total magnetization and thickness, $J_t\varepsilon$, were evaluated for geologic units Tma and Tmr along the Yucca fault by computing the theoretical anomalies that compare favorably with the downhole anomalies on figure 7. Computations using a three-dimensional program give downhole anomalies with large and abrupt changes at tops and bottoms of uniformly magnetized units. Within the unit, the theoretical anomaly is constant and can be represented by a straight line. Magnetizations are seldom uniform, and it is therefore necessary to convert downhole anomalies to a format consisting of several straight-line segments to provide a basis for comparisons with theoretical anomalies. Figure 8 shows the four segments that represent downhole anomalies from the Tma ash-flow tuff, and the eight segments that represent inhole anomalies from the Tmr ash-flow tuff. Calculated magnetization-thickness products, $J_t\varepsilon$, are given for each segment. By summing individual products, the average for $J_t\varepsilon$ is 25 A for Tma, and 263 A for Tmr. These are the values we used for analysis of air and ground magnetic anomalies at the Yucca fault.

Anomaly Analysis

The almost complete geologic description of the Yucca fault, and its good definition by aeromagnetic anomalies, offers an unparalleled opportunity for calibration of interpretive methods. The fault is still active and its trace is marked by a topographic feature in the surficial deposits (Fernald and others, 1968). Depths to the Rainier Mesa and Ammonia Tanks Members of the Timber Mountain Tuff in drill holes on both upthrown and downthrown sides of the fault are given by Dixon and others (1975). The anomalies extend in a belt from south to north (fig. 6), and amplitudes vary from less than 20 to 216 nT.

Two simple ratios using distances between anomaly maximum and minimum, $|Xmax - Xmin|$, were developed to approximate depth to center of a magnetized flow on the upthrown side of a normal fault, h, and position of its trace, Xo, along east-west traverses. The depth is given by

$$Rh = \frac{|Xmax - Xmin|}{h} , \qquad\qquad (1)$$

and the trace by

$$Rt = \frac{|Xo - Xmin|}{|Xmax - Xmin|} . \qquad\qquad (2)$$

The ratios may result from geological interpretations, Rhg and Rtg, or anomaly analysis, Rha and Rta. The ratios provide a rapid and convenient method to help identify the principal anomaly-producing flow, and to map its position beneath the surface.

A

Magnetic Anomaly, in nT

$J_t \epsilon = 7.0A$

$J_t \epsilon = 9.2A$

$J_t \epsilon = 6.5A$

$J_t \epsilon = 2.8A$

B

Magnetic Anomaly, in nT

$J_t \epsilon = 7.7A$

$J_t \epsilon = 45.2A$

$J_t \epsilon = 37.6A$

$J_t \epsilon = 57.7A$

$J_t \epsilon = 42.7A$

$J_t \epsilon = 41.1A$

$J_t \epsilon = 19.2A$

$J_t \epsilon = 11.8A$
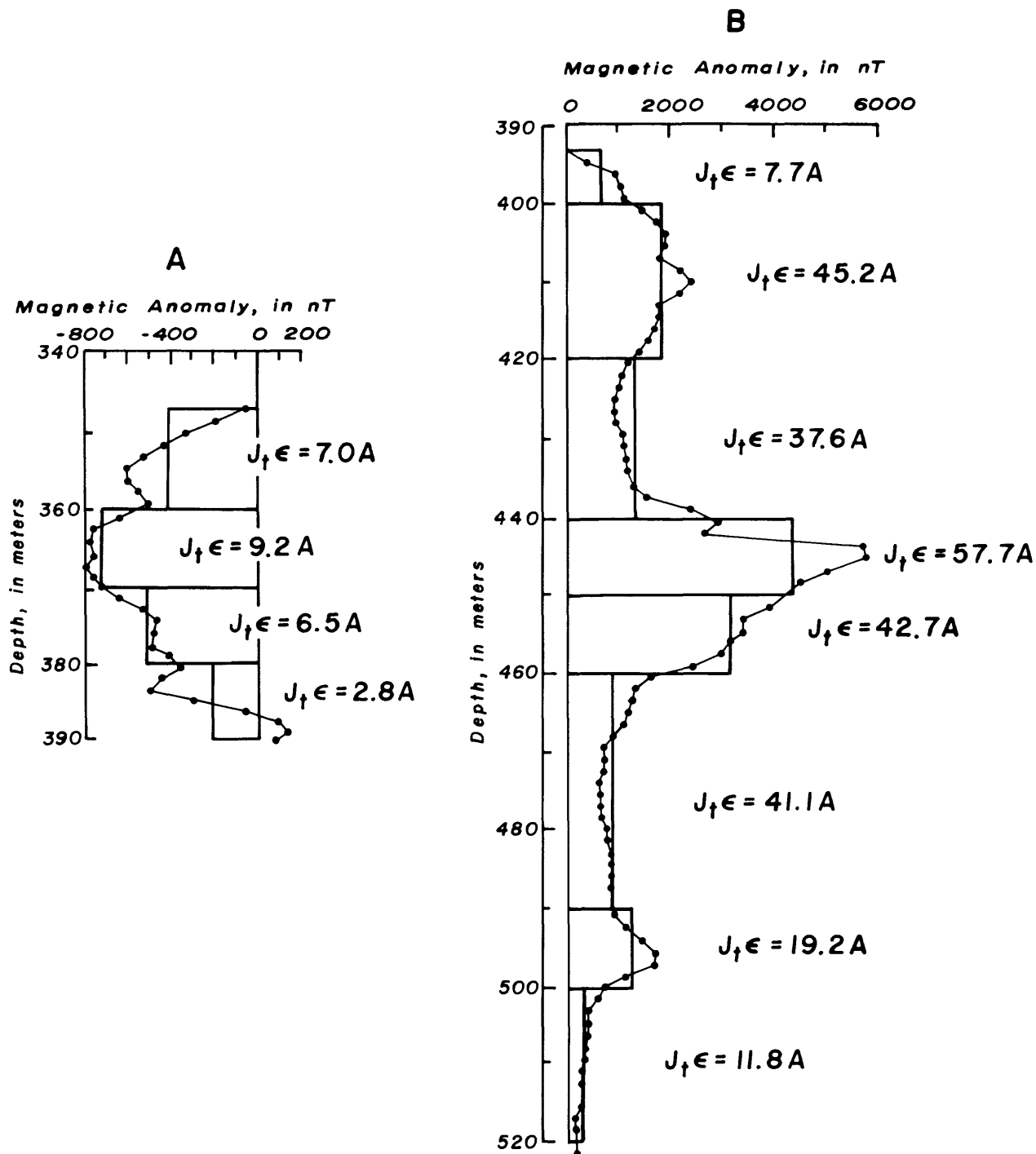
Figure 8.--The anomalies from figure 7 converted into four straight-line
segments (A) representing the effects of Tma, and eight straight-line
segments (B) representing the effects of Tmr. Computed values of
magnetization-thickness product, $J_t \epsilon$, are given for each segment. $J_t \epsilon$ is
represented by the area between the anomaly and the depth axis.

18

Geologic ratios have been computed for 15 aeromagnetic traverses, 8 north of ground traverse E67-E67' (fig. 6), and 7 south of the traverse. Over this interval, the depth to Tmr ash-flow tuff on the upthrown side increases from a mimimum of 77 m (250 ft) near E67-E67' to maxima of about 200 m (655 ft) near the south and north quadrangle borders, and the vertical throw of the fault decreases from south to north from about 400 m (1,300 ft) to 200 m (650 ft). Depths and throws were estimated by using planar surfaces to represent Tmr on the high and low sides. A high-side plane dipping 16° southwest was determined by a least-square adjustment of 15 drill-hole depths, and low-side plane dipping 4° southwest by an adjustment of 6 drill-hole depths. The position of the fault trace shown on figure 6 is beneath the maximum slope of the anomaly indicated by the contours. Averages and standard deviations for |Xmax - Xmin| are 510 m (1,675 ft) ± 104 m (340 ft) (15), for Rhg 1.95±0.23 (15), and 0.47±0.11 (15) for Rtg.

The two-dimensional inverse program was applied to anomalies along truck traverse E67-E67' to compare interpreted with known fault structure, and to compare analysis with geologic ratios. Traverse E67-E67' was selected to investigate effects arising primarily from the upthrown side of the fault. Its depth here is only 77 m (250 ft) whereas the depth on the downthrown side is 360 m (1,180 ft). Results of the analysis are an interpreted structure similar to known structure, interpreted magnetic properties similar to known properties, and Rha = 2.04 and Rta = 0.42. KPQ analysis of the 522 nT anomaly designated a two-dimensional magnetized sheet on the upthrown side as the primary source. As shown on figure 9, the sheet has a headpoint at traverse station 1,790 m (5,875 ft); depth, h, of 70 m (230 ft); magnetization angle, β, of 105°; $J_t \varepsilon$ = 183 A; and an unknown geologic dip angle, θ . As pointed out by Karl Jung (1953), the same anomaly can be produced by θ = 0° representing a normally magnetized horizontal flow extending east of the fault, by θ = 110° representing a near-vertical dike with intermediate direction of magnetization, by θ = 180° representing a reversely magnetized horizontal flow extending west of the fault, etc. The latter case was accepted because it is consistent with the geologic dip of 16° southwestward (θ = 164°) known from drill-hole data, and with the direction of total magnetization known from measurements of oriented samples of the Rainier Mesa Member collected from its type locality on Rainier Mesa near A on figure 1.
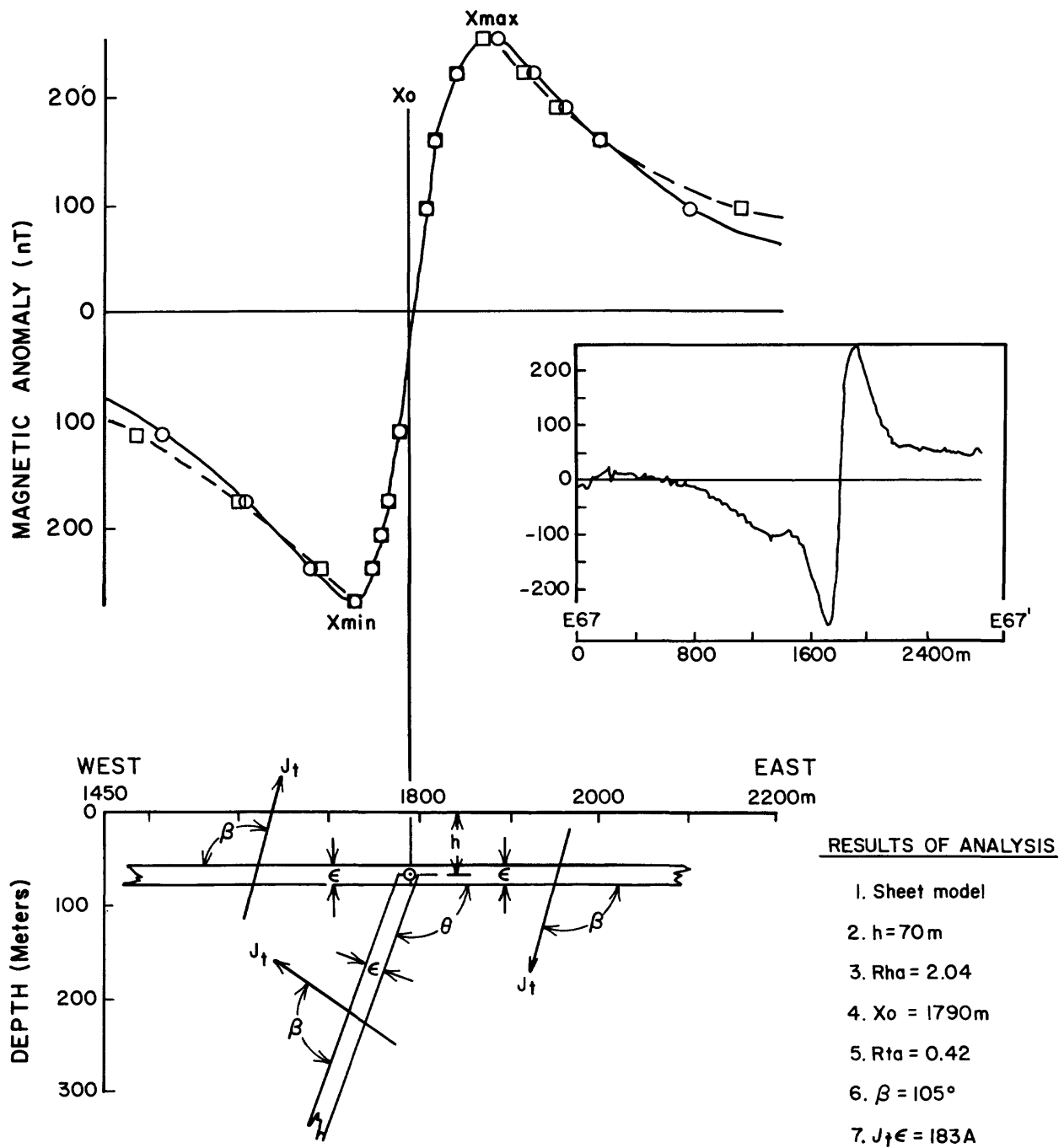
19

Figure 9.--Inversion analysis of residual anomaly along part of truck traverse
E67-E67'. Entire traverse is shown in insert. Solid line is residual
anomaly, and dashed line is theoretical anomaly for a sheet model.
Circles are conjugate points for the residual anomaly, and squares are
conjugate points for the theoretical anomaly. Symbols are described in
the text.

20

Similar results were found by applying the KPQ method to the 15 aeromagnetic traverses of figure 6. Depths and magnetization angles designated the Tmr flow on the upthrown side of the fault as the probable source. Analysis ratios were similar to geologic ratios: Rha = 2.07±0.21 (15), and Rta = 0.46±0.08 (15). Effects from the Tmr flow on the downthrown side reduced anomaly amplitudes, and thus $J_t\varepsilon$ values were less than the 263 A from drill hole U4e-1. They averaged 145 A ± 30 A (15).

The effects of increasing vertical displacement of the Yucca fault in air anomalies along traverse E67-E67' were investigated by using a three-dimensional forward program to compute anomalies from simple models. The geologic and magnetic property input for Tma are ε = 43 m (140 ft), J_t = 0.58 A/m with azimuth = 0° and inclination = 59°; and for Tmr are ε = 127 m (415 ft), J_t = 2.07 A/m with azimuth = 168 and inclination = -55°. Figure 10 shows anomalies for displacements of 180 m (590 ft), 270 m (886 ft), 360 m (1,181 ft), 540 m (1,772 ft), and for high side only (∞ displacement). Larger displacement increased anomaly amplitude from 75 to 144 nT, $J_t\varepsilon$ from 92 to 176 A, and Rhg from 1.41 to 2.00. Also, calculations indicate a vertical displacement of 45 m (150 ft) is required to produce a significant anomaly amplitude of 20 nT. There was no important change in Rtg.

YUCCA MOUNTAIN AREA

Application of the technique developed at Yucca Flat to aeromagnetic anomalies in the Yucca Mountain area identifies the Topopah Spring Member of the Paintbrush Tuff (Tpt) as the primary source and maps traces of major fault structures that have vertical displacements greater than 70 m (230 ft). The Tpt ash flow is normally magnetized, deposited over much of NTS, and present in all of the Yucca Mountain area. Detailed measurement of magnetic properties of drill-core samples designates several other volcanic units as potential anomaly producers. The regional structure consists mainly of several faulted blocks of volcanic rock dipping at low eastward angles (Lipman and McKay, 1965; Christiansen and Lipman, 1965) that produce north-south alinements of positive and negative anomalies. No major magnetized structure crosses the site in the north-south direction, but one east-west trend of anomalies extends across the (D of figs. 2 and 11) central part. The trend is not uniform and is not completely defined in the east-west air traverses. North-south air and ground traverses were therefore measured to obtain better anomaly resolution. Most of the trend across the site is eliminated by removing the magnetic effects of the deep source.

Vertical displacement (m)	Rhg	Rtg
180	1.41	0.45
270	1.55	0.50
360	1.66	0.47
540	1.77	0.44
∞	2.00	0.48
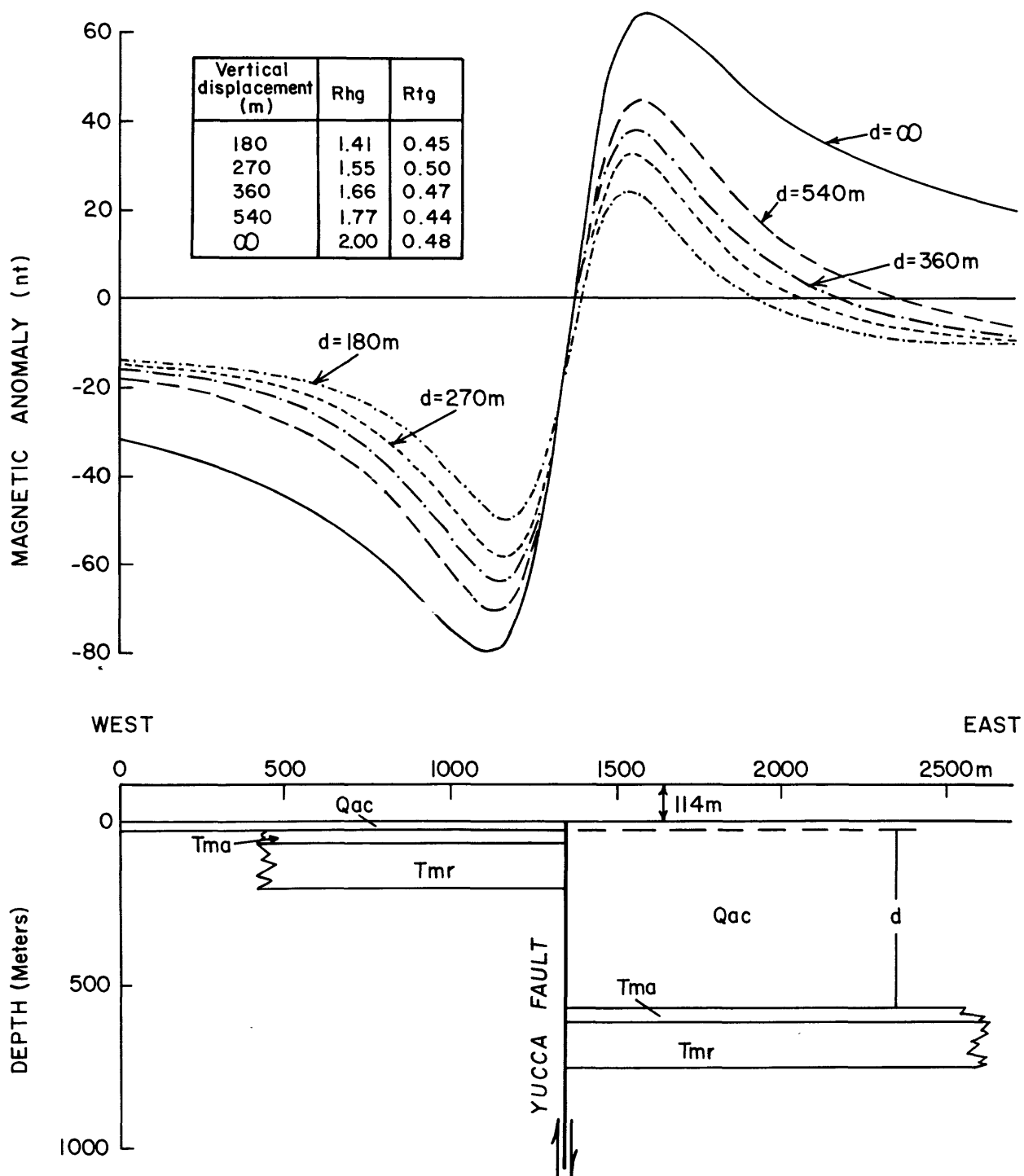
Figure 10.--East-west section along traverse E67-E67' showing aeromagnetic anomalies, and Rhg and Rtg values, computed for simple models that represent an increase in vertical displacement at the Yucca fault. Displacements increase from 180 m (590 ft) to the maximum (∞) that eliminates entirely the magnetic effects of the low-standing side of the fault.

22

Figure 11.--Residual aeromagnetic map of Yucca Mountain area showing complex effects of volcanic rocks superimposed on deeper effects of magnetized sedimentary rocks. Also shown are the site area (shaded), areas A, B, C, and D of figure 2, air traverses F77-F77' and G77-G77', and five drill holes. Hachures indicate zero contours and closed areas of lower magnetic intensity.

Contour interval = 100 nT   Measurements 120 m (400 ft) above surface

Low-Altitude Survey

The residual anomalies shown on figures 11 and 12 (in pocket) were compiled by adding 350 nT to the 1977 International Geomagnetic Reference Field (IGRF) for aeromagnetic maps published for most of NTS (USGS, 1979). The 350 nT is the difference between the IGRF datum and our reference surface in the Mercury area. The survey was along east-west traverses about 400 m (1,320 ft) apart and 120 m (400 ft) above the surface.

The contours of figure 11 show a complex pattern of anomalies arising from local effects of volcanic rock added to regional effects of magnetized Eleana Formation. Average values are related to the deeper source and increase northward from about zero near the southern border to about 200 nT over the northern part of the proposed site. Examples of combined effects are the maxima of 503 nT near A, 497 nT near·B, and 652 nT near C. The east-west trend of anomalies crosses the site near D where contour values increase from about 100 to 200 nT.

Magnetic Properties And Theoretical Anomalies

Large changes in total magnetization varying from nonmagnetic to strongly magnetic, and both normal and reversed polarities, were found in the large number of surface and drill-core samples of volcanic rock measured by J. G. Rosenbaum (written commun., 1983). Magnetic properties and data from geologic exploration drill holes USW G-1 (Spengler and others, 1981), USW G-2 (Maldonado and Koether, 1983), and USW G-3 (Scott and Castellanos, written commun., 1982) suggest the following seven units as possible anomaly producers:

Tiva Canyon Member of Paintbrush Tuff (Tpc)
Pah Canyon Member of Paintbrush Tuff (Tpp)
Topopah Spring Member of Paintbrush Tuff (Tpt)
Bullfrog Member of Crater Flat Tuff (Tcb)
Tram unit of Crater Flat Tuff (Tct)
Lava flow and flow breccia (Tfb)
Lava and flow breccia. (Tll)

The younger Rainier Mesa Member is present locally in the area but occupies relatively small areas at the foot of fault blocks and was penetrated only in drill hole UE25p-1 (M. D. Carr, written commun., 1983). The holes are shown on figures 2 and 11, and the geologic units are shown in section on figures 4 and 5.

24

Table 1.--Magnetic properties and thicknesses of four ash flows that were penetrated in drill holes USW G-1, USW G-2, and USW G-3 (from J. G. Rosenbaum, written commun., 1983).

Unit	Drill hole	Polarity	$J_t\epsilon$ (A/m)	ϵ (m)	$J_t\epsilon$ (A)
Tpt	USW G-1	Normal	1.3	335	469
Tcb	USW G-1	Normal	1.0	130	130
Tct	USW G-1	Reversed	1.2	268	322
Tpt	USW G-2	NNormal	1.4	285	399
Tcb[1]	USW G-2	Normal	0.2	128	26
Tct[1]	USW G-2	Reversed	0.2	100	20
Tpc	USW G-3	Reversed	0.9	103	93
Tpt	USW G-3	Normal	1.2	272	326
Tcb	USW G-3	Normal	3.0	182	546
Tct	USW G-3	Reversed	1.8	369	664

[1] Altered samples.

Four ash-flow tuff units that range in age from about 14 to 12 m.y., Tct, Tcb, Tpt, and Tpc, are continuous and relatively uniform throughout the site area, and, therefore, produce predictable magnetic anomalies. Their magnetic properties and thicknesses are given in table 1. The reversely magnetized Tpc crops out over most of the site area, and due to erosion, its thickness may vary from zero to about 120 m (400 ft). Thickness is more constant for the normally magnetized Topopah Spring ash-flow tuff, ranging from 285 m (935 ft) to 335 m (1,100 ft) and averaging 307 m (1,007 ft). Magnetization of the Topopah in the three holes is moderate and averages 1.3 A/m, and magnetization-thickness products are high and average 398 A. Thicknesses and magnetizations are much more variable for the units buried at greater depths. Their magnetization-thickness products vary from 20 to 664 A, with Tcb averaging 234 A and Tct averaging 335 A.

The drill holes provided the input data for developing simple two-dimensional models to represent configurations of flows along vertical faults striking north-south and east-west. Theoretical anomalies can then be computed with the forward program for the models, and compared with observed anomalies in the Yucca Mountain area. The units appear to dip at low angles, and a horizontal attitude was assumed for the models. A plane adjusted to the top of the Topopah Spring Member strikes N. 3° W. and dips only 6° eastward. Seven points were used in the least-square adjustment, three from drill-hole data and four from outcrop data. Also, it was assumed that the volcanic section at the site can be represented by the thicknesses and magnetic properties of tuff units cored in hole USW G-1. In the models, Tpc has a thickness of 91 m (300 ft) and a total magnetization of 1.1 A/m. Azimuths and inclinations of total magnetization are 167° and -38° for Tpc, 326° and 62° for Tpt, 13° and 49° for Tcb, and 141° and -42° for Tct. Azimuths are measured clockwise from north, and inclinations are measured positive downward from horizontal.

Figure 13 shows in sectional views the individual and total anomalies caused by unit edges that were formed by infinite displacement of vertical faults striking both east-west (A) and north-south (B). The illustration gives anomalies at the aeromagnetic datum along edges extending south from an east-west fault, and extending east from a north-south fault. But the anomalies will also apply to edges extending in opposite directions when anomaly sense is changed by a rotation of 180° about the zero anomaly line.
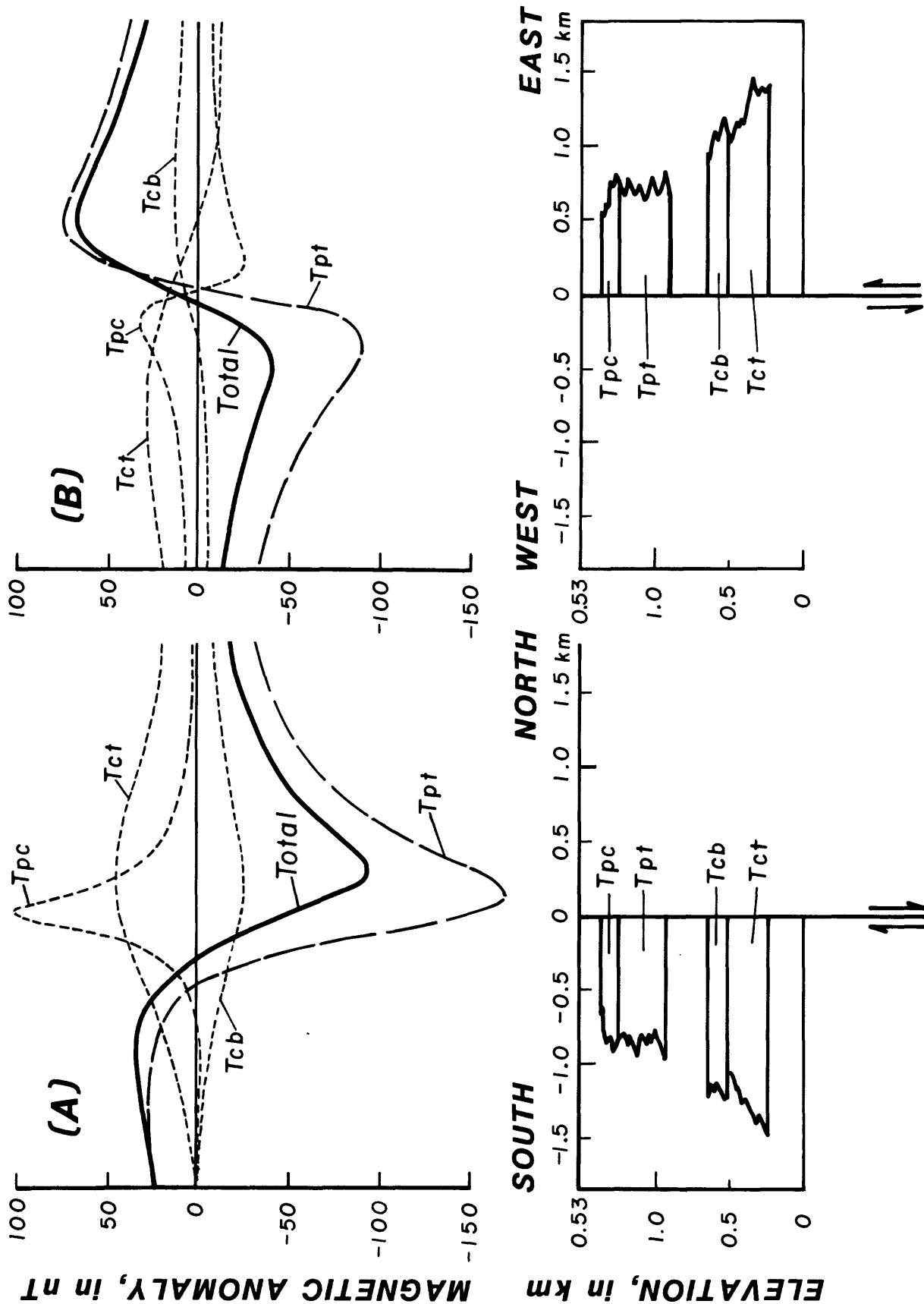
Figure 13.--Cross sections showing theoretical anomalies for individual effects of flows Tct, Tcb, Tpt, and Tpc, and their total effect at a vertical fault. The fault strikes (A) east-west over flows extending south, and (B) north-south over flows extending east.

27

Inspection of anomaly configuration on figure 13 reveals that shapes of the total anomalies resemble the individual anomaly computed for Tpt, and resemble the observed anomalies found in the Yucca Mountain area over north-south faults (fig. 12). But significant differences were found in application of the KPQ method. Reliable parameters of geometry and magnetization of the model were recovered only from the Tpt anomaly. However, results of application to the combined anomaly were satisfactory for position of fault trace and depth to center of Tpt. Ratios for the total anomaly from a north-south fault are similar to those found in Yucca Flat: Rhg = 1.96 and Rtg = 0.52. The extreme points on anomalies from the east-west fault are too poorly defined to apply the ratio rules.

Figure 14 shows in sectional view the total anomalies caused by flow edges that were formed by increasing the amount of vertical displacement along a north-south fault down to the west. The anomalies also apply to down-to-the-east displacements by rotating anomalies 180° about their zero lines. Increasing displacements from 100 m to infinity increased anomaly amplitudes from 26 to 111 nT, $J_t\varepsilon$ from 58 to 247 A, and Rhg from 1.51 to 2.00, and caused no real change in Rtg. A vertical displacement of 70 m (230 ft) is required to produce a significant aeromagnetic anomaly.

Relation Of Anomalies To Faults

Anomaly analysis designates the Topopah Spring Member Tuff as the main anomaly producer in the Yucca Mountain area; and designates five named faults as major structures, and six other major structures that have less extensive strike lengths. Major structures are defined as those having the required aeromagnetic map of Kane and Bracken (1983) and the 1:62,500 aeromagnetic maps of the U.S. Geological Survey (1979).

The basis for mapping fault traces is identification of the Tpt unit as the primary source of air anomalies. The KPQ method was applied to four anomalies over the fault of Solitario Wash on traverse F77-F77' (fig. 11) and three adjacent traverses to the north, and to three anomalies over the fault of Windy Wash on traverse G77-G77' (fig. 11) and two adjacent traverses to the south. For geologic control, all traverses were selected in areas where the Tpt unit crops out (fig. 15, in pocket) along topographic highs just east of the faults. Also, traverse F77-F77' is over drill hole USW G-3, which penetrated 272 m (892 ft) of Tpt. The analyses, plus input for a low eastward dip from geologic mapping, indicates two possible two-dimensional models that are sheet-like in configuration. As illustrated on figure 16 for the anomaly on traverse F77-F77', one is at a shallow depth and has a horizontal west edge that could result from erosion, and the other is at twice the depth and has a vertical west edge that could result from faulting. Inclination and azimuth of total magnetization of both are similar to those in oriented samples of Tpt.

28

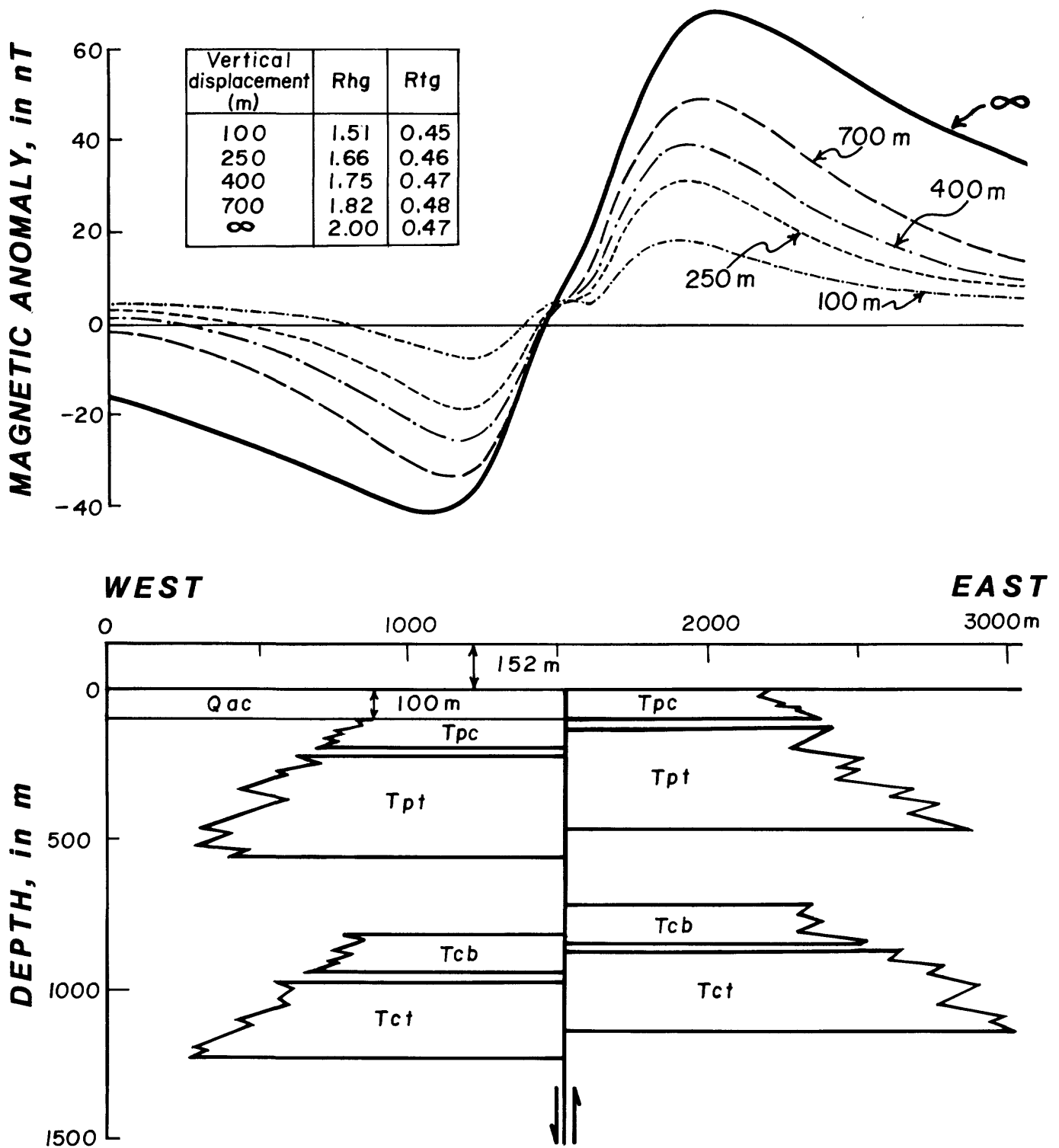| Vertical displacement (m)	Rhg	Rtg
100	1.51	0.45
250	1.66	0.46
400	1.75	0.47
700	1.82	0.48
∞	2.00	0.47

Figure 14.--Cross section showing theoretical anomalies for total effect of Tct, Tcb, Tpt, and Tpc flows at a fault that strikes north-south and has an increasing vertical displacement down to the west.

29

The deeper model gives a more credible designation of Tpt as primary source because its configuration is more reasonable, its depth is similar to that of strongly magnetized rock in the lower part of the Tpt unit (J. G. Rosenbaum, written commun., 1983), and its depth ratio is close to those at the Yucca fault. The four anomalies over the fault at Solitario Wash give an average depth of 203 m (666 ft) from KPQ analysis and 204 m (670 ft) from the average depth ratio of 2.13; and average inclination and azimuth of total magnetization of 69° and 326°. The three anomalies over the fault at Windy Wash give an average depth of 287 m (942 ft) from KPQ analysis and 286 m (945 ft) from the average depth ratio of 1.99; and average inclination and azimuth of total magnetization of 40° and 326°.

The insert on figure 16 shows several anomalies along traverse F77-F77' can be explained by edge effects of the Topopah Spring Member. The 285 nT anomaly at A is from the fault at Solitario Canyon down to the west, the 122 nT anomaly at B is from fault C down to the east, the 66 nT anomaly at D is from fault D down to the east, and the 80 nT anomaly at E is from fault E down to the west. The anomaly with an amplitude of 87 at C is also fault related. The larger amplitude at A is probably due to both greater fault displacement and the presence of reversely magnetized rock of the Rainier Mesa Member (Tmr) on the downthrown side of the fault at Solitario Canyon. Measurements of magnetic properties of 24 roughhewn samples by the method of Jahren and Bath (1967) assign the ash flow a moderate magnetization that averages 1.12±1.33 A/m (24). But this relatively young unit is not continuous throughout much of the area, and is mostly draped over rather than displaced by the faults.

A detailed contouring of low-altitude aeromagnetic data for the Yucca Mountain area is given on figure 12 at the 1:24,000 scale of the quadrangle maps by Lipman and McKay (1965) and Christiansen and Lipman (1965), and a work-sheet map of the same area is given on figure 15. The contoured map shows paths of all east-west flight lines and the anomaly trends that were selected to define major structural trends. The work sheet shows the relation of interpreted positions of the 11 major faults to the points of maxima and minima anomaly, the 10 drill holes, and the outcrops of Topopah Spring Member and Rainier Mesa Member. The positions of interpreted edges of the Topopah Spring Member usually follow in a continuous direction the fault traces that are known or inferred from geologic mapping. Abrupt deviations in trends of these edges can result from offsetting effects of east-west structures, changes in stratigraphy or magnetic properties of volcanic units, or from errors in plotting the position of the airplane. Near the western border of the site, the trace of the Solitario Wash fault is given as N. 8° E. by anomalies along 19 flight lines on figure 12, but there is one offset to the west near D on figure 11. The offset anomaly is part of the east-west trend of anomalies that crosses the central part of the site. Interpretations designate the Tiva Canyon Member as the source of anomalies along the dashed line on figure 15 north of the site at Drill Hole Wash. The anomalies are caused by the severe topographic effects of the wash.
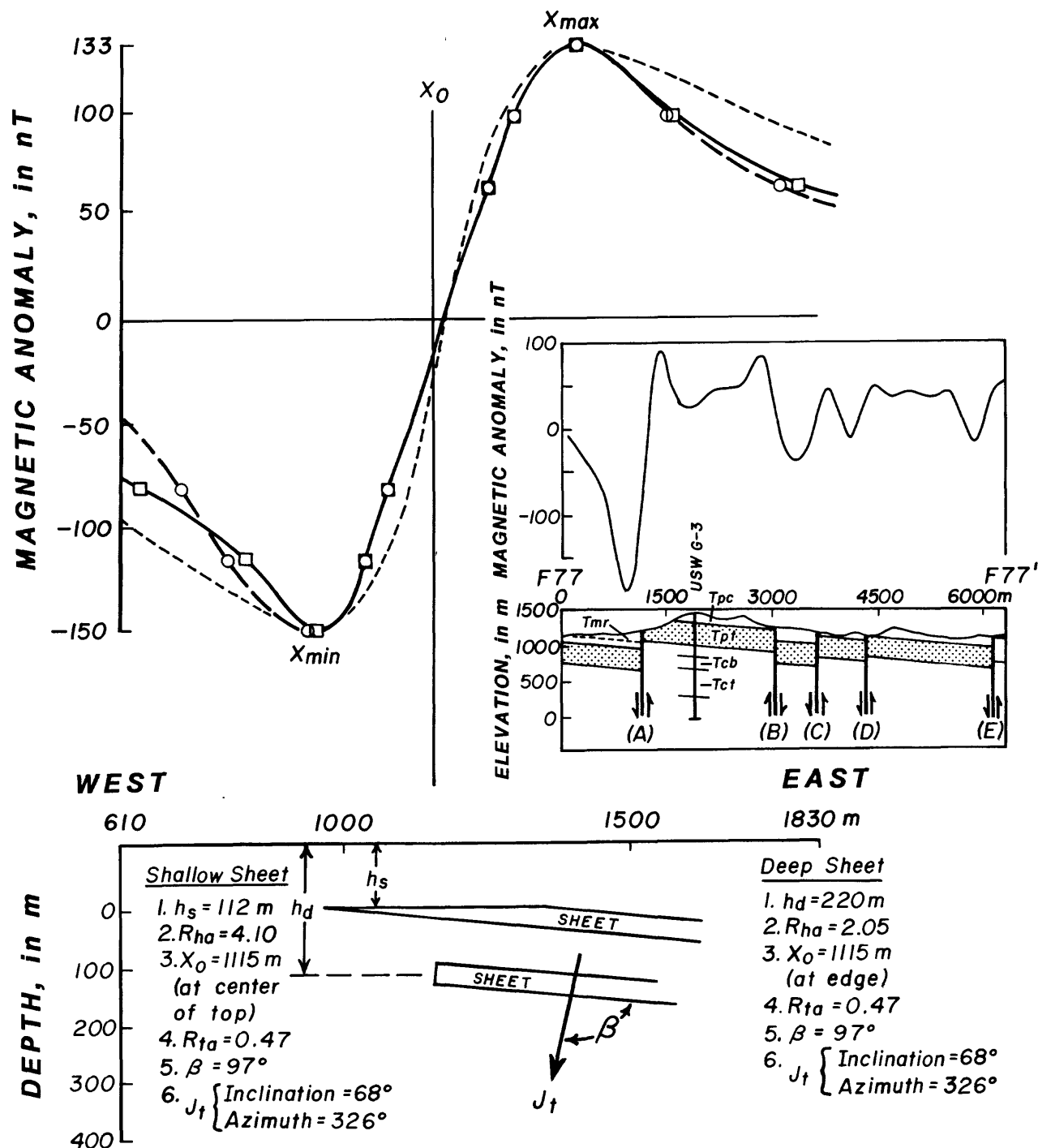
Figure 16.--Inversion analysis of residual anomaly over fault at Solitario Wash along part of air traverse F77-F77' giving comparisons of residual anomaly (solid line) with anomalies computed for shallow (dashed line) and deep (dotted line) sheets that are 37 m (120 ft) thick, dip 6° eastward, and have the same magnetizations. Insert shows in section the entire traverse of figure 11; and the Tpt unit (shaded) as displaced by the fault at Solitario Wash (A), fault C (B), a minor fault (C), fault D (D), and fault E (E) on figure 15.

Relation Of Anomalies To East-West Structure

The possibility of an east-west structure crossing the site is reinforced by the residual anomalies shown on figure 17 (in pocket) that were compiled from aeromagnetic data measured along lines flown in north and south directions. The lines are about 400 m (1,320 ft) apart and 120 m (400 ft) above the surface. A constant of 500 nT was added to the 1980 IGRF to tie the new survey to the datum of figures 11 and 12. Figure 17 is the result of adding 500 nT to contours that were generated by computer for values at grid intervals of 250 m (820 ft). Contours conform better with original measurements in a compilation for a smaller area (fig. 18) that includes the central part of the site. A constant of 510 nT was added to the IGRF datum, and contours were adjusted to the continuous data along 13 flight lines.

The general distribution of contours is similar on figure 12 (1:12,000 scale) and figure 17 (1:48,000 scale), and differences in detail become plausible after considering differences in position and direction of flight paths. The contours of the new survey are positioned near the previously interpreted faults (fig. 19, in pocket), and show isolated anomalies from volcanic rock sources and a northward increase in average value from the deep source. A good definition of east-west trends was obtained, and a few unexpected anomalies were revealed. An example of the latter is the isolated positive anomaly over the Topopah Spring Member near the western boundary of the site, best shown as the 290 nT minimum on figure 18. Its source is probably an abrupt increase of magnetization within the Topopah Spring or Bullfrog Member, but it could be a small intrusive feature at shallow depth.

Ground magnetic anomalies along traverses H82-H82', I82-I82', and J82-J82' (figs. 20, 21) were measured at 3-m (10-ft) intervals to investigate continuity of east-west features, anomalies remaining after effects of the deep source were removed, and magnetization of outcropping units or those beneath a thin cover of alluvium. The zero datum near Mercury was brought into the area by repeated measurements at base stations and making corrections for planar regional field of the aeromagnetic surveys. The data indicate most residual anomalies come from small features having limited extent in their east-west direction. This was determined by comparing anomalies smoothed by continuation upward to 120 m (Henderson and Zietz, 1949) with anomalies shown on figure 18 that were measured 120 m above the surface. This also is true for anomalies that remained after the deep-source anomaly was removed. Amplitudes of residual anomalies indicate magnetizations vary from weak to strong for Rainier Mesa Member along traverse H82-H82' (fig. 20) and Tiva Canyon Member along traverses I82-I82' and J82-J82' (fig. 21).
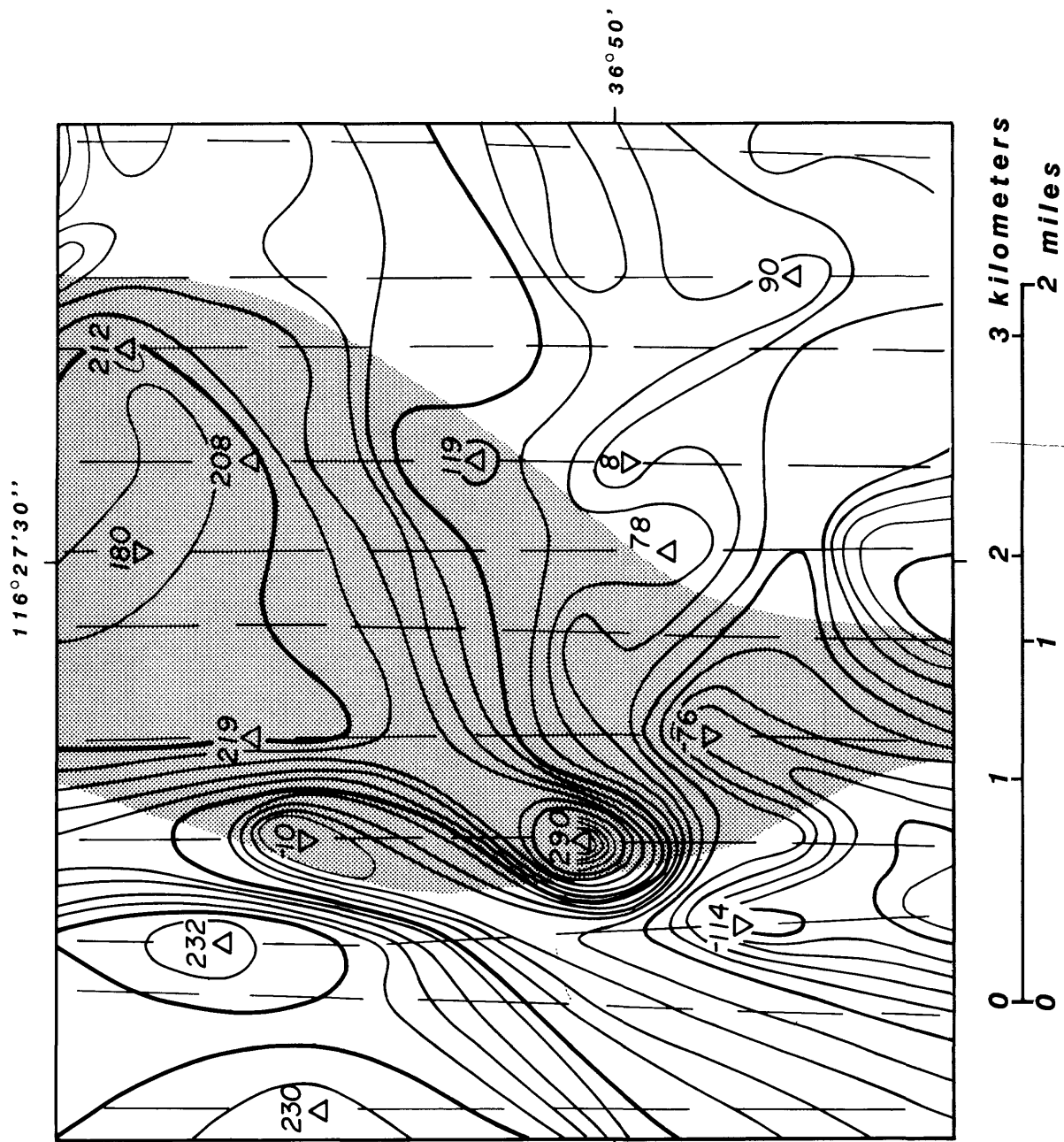
Contour interval=20 nT   Measurements 120m(400ft) above surface

Figure 18.--Residual aeromagnetic map of central part of site showing an increase of more than 100 nT in contours near (A) extending northeast across the site. Contours were adjusted to continuous data along flight lines. Also shown are values of maxima and minima along lines, and the site area (shaded).
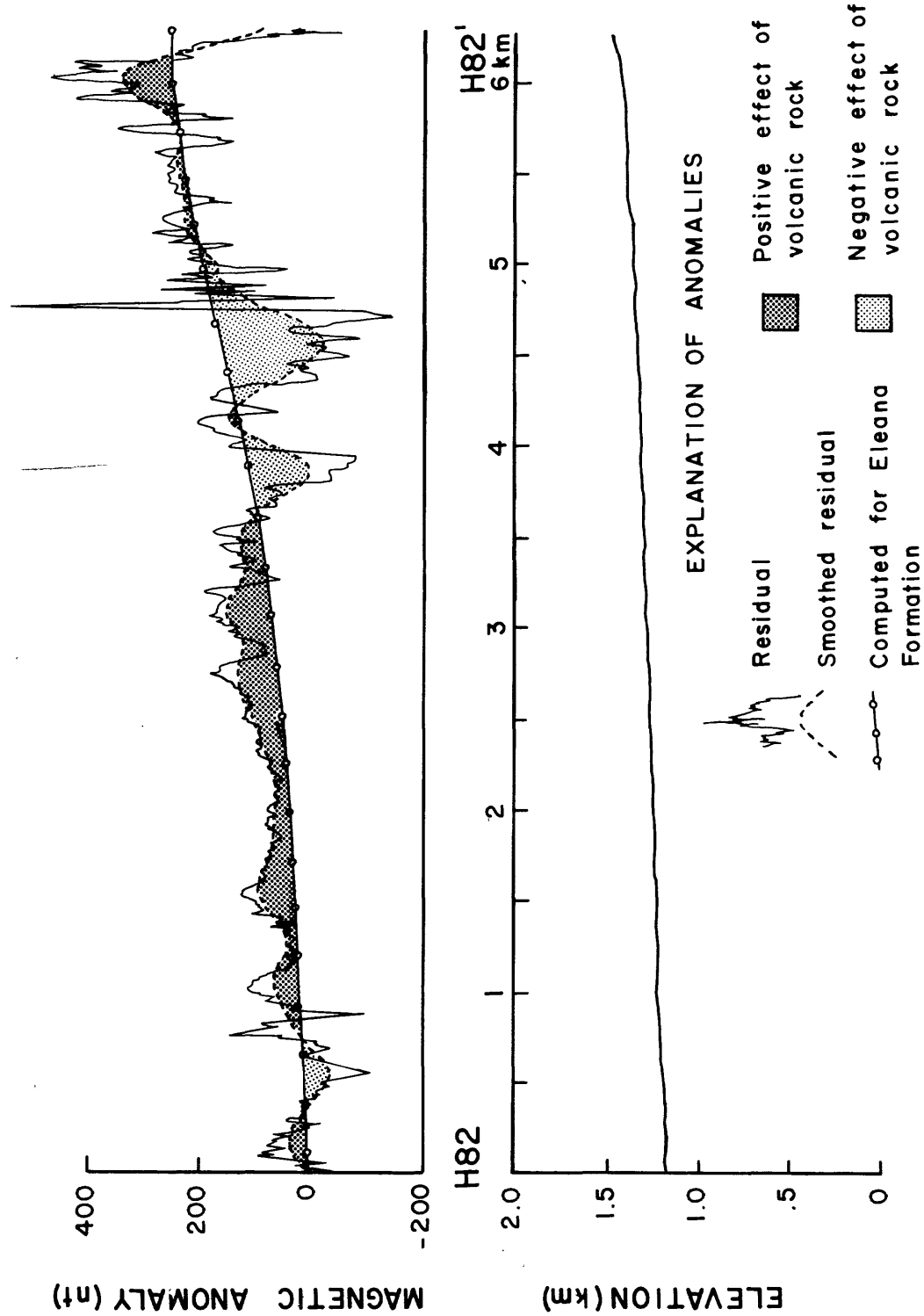
33

Figure 20.—Anomalies along ground traverse H82-H82' (fig. 19) showing positive and negative anomalies that result when effect of deep source is subtracted from smoothed residual anomalies.
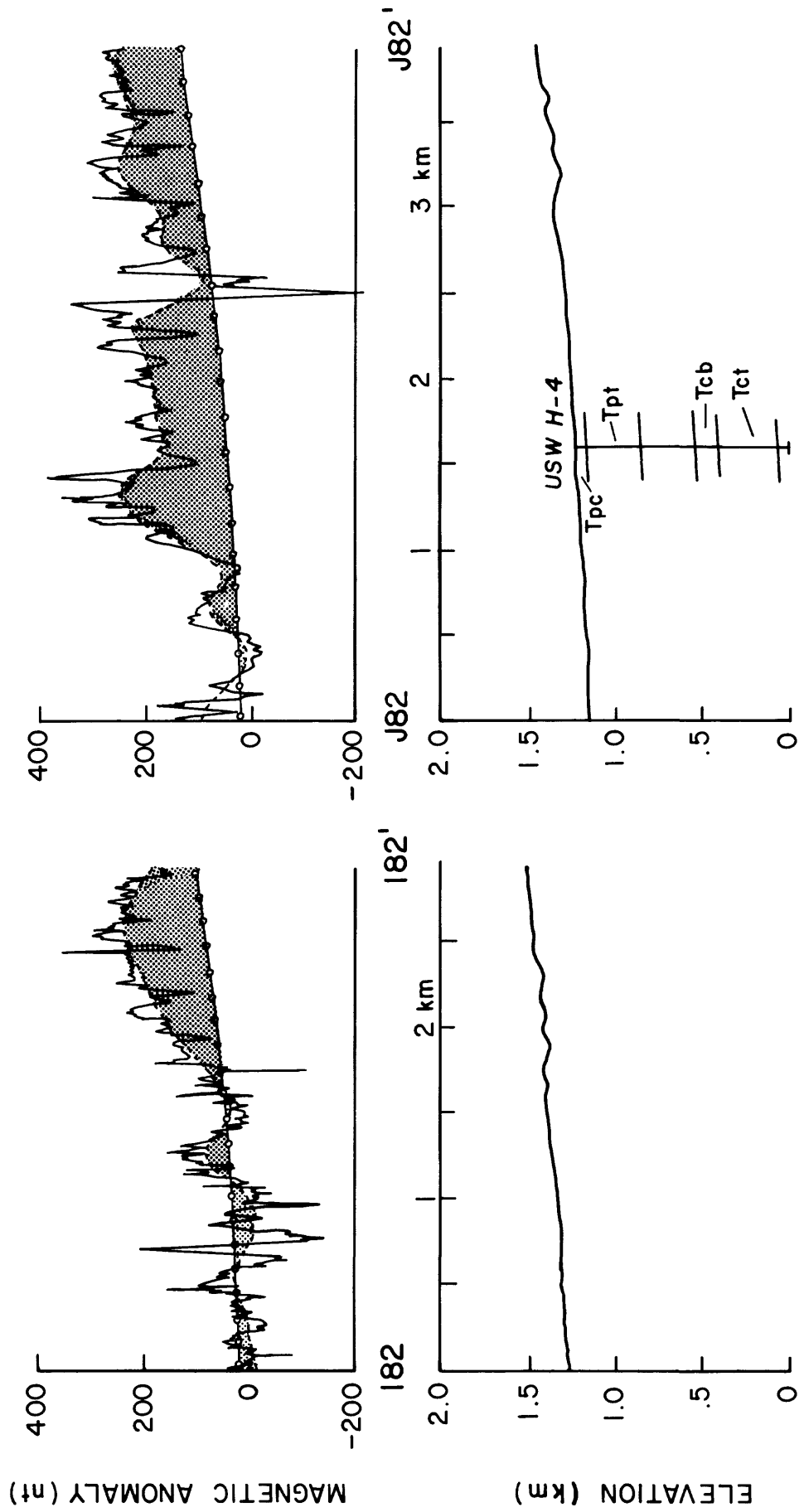
34

Figure 21.--Anomalies along ground traverses I82-I82' and J82-J82' (fig. 19) showing positive and negative anomalies that result when effect of deep source is subtracted from smoothed residual anomalies.

35

The aeromagnetic contours on figure 18 show an anomaly striking northeast across the site that is not removed entirely by subtracting the anomaly from the deep source. The amplitude of more than 100 nT on figure 18 is reduced to about 40 nT on figure 22. Depth estimates (Vacquier and others, 1951) place the source beneath the Topopah Spring Member but within the volcanic section. As shown on figure 13 (A), a positive anomaly striking east-west can be produced by the north edge of a reversely magnetized unit like the Tram Member of the Crater Flat Tuff. It also can be produced by the south edge of a normally magnetized unit like the lava flow found in drill holes north of the anomaly, but not found south in drill hole USW G-3. The latter possibility is strengthened by the increase in thickness and intensity of magnetization of normally magnetized dacite flows found in drill holes USW H-5 and USW H-6 (fig. 15) below the Tram Member. The total magnetization of 24 samples of dacite collected in USW H-6 from depths of 915 m (3,000 ft) to 1,100 m (3,610 ft) vary from 0.09 to 5.00 A/m (J. G. Rosenbaum, written commun., 1983) and the magnetization-thickness product is 180 A.
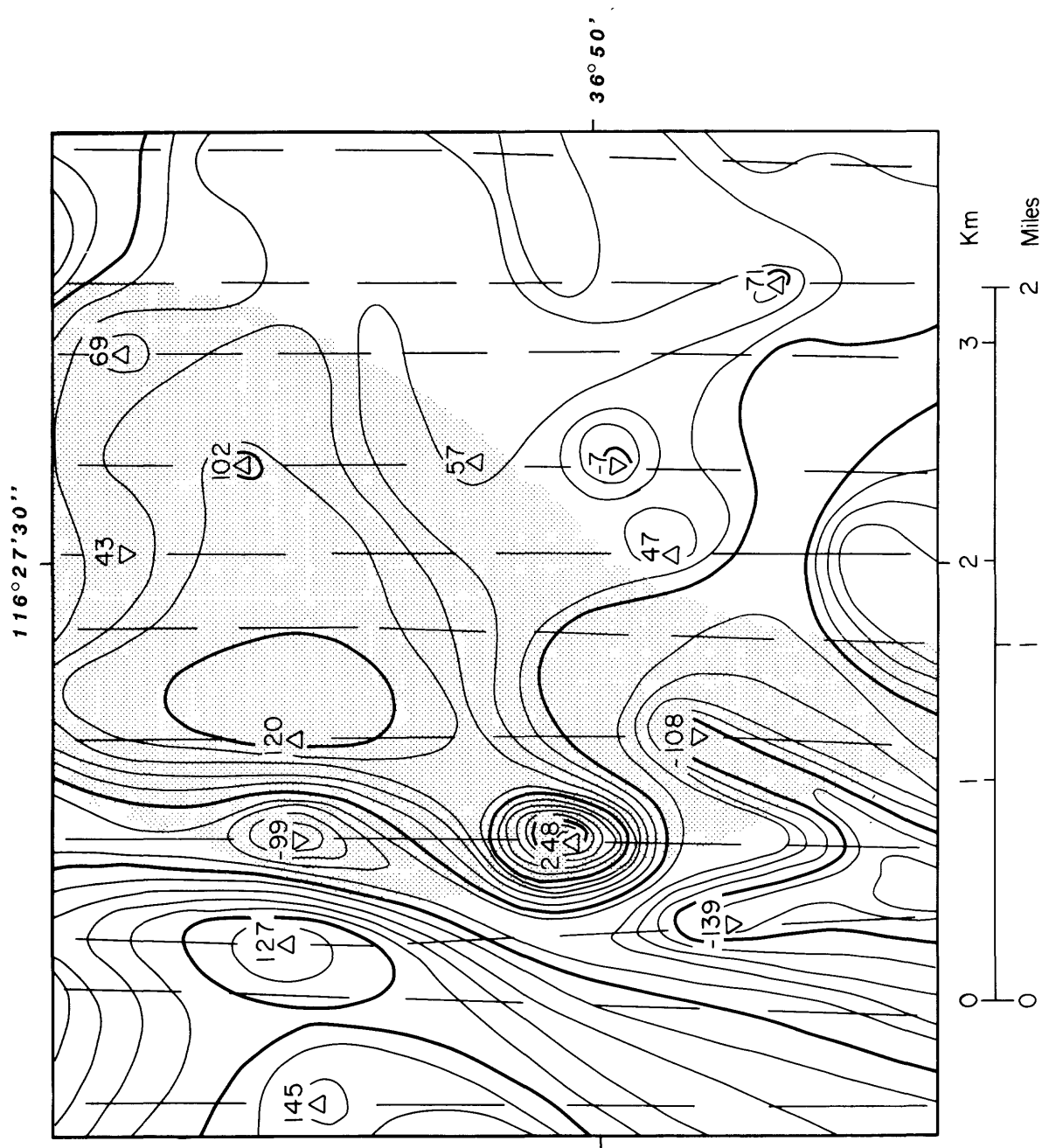
Contour interval = 20nT   Measurements 120m (400ft) above surface

Figure 22.--Residual aeromagnetic map of central part of site showing that removal of deep effect from data (fig. 18) decreases amplitude of northeast trend at A to about 40 nT. Also shown are values of maxima and minima along lines, and the site area (shaded).

37

REFERENCES CITED

Baldwin, M. J., and Jahren, C. E., 1982, Magnetic properties of drill core and surface samples from the Calico Hills area, Nye County, Nevada: U.S. Geological Survey Open-File Report 82-536, 27 p.

Bath, G. D., 1968, Aeromagnetic anomalies related to remanent magnetism in volcanic rock, Nevada Test Site, Nevada, in Nevada Test Site: Geological Society of America Memoir 110, p. 135-146.

_____1976, Interpretation of magnetic surveys in intermontane valleys at Nevada and southern New Mexico: U.S. Geological Survey Open-File Report 76-440, 36 p.

Bath, G. D., Dixon, G. L., and Rosenbaum, J. G., 1982, Relation of aeromagnetic anomalies to faulted volcanic terrains at the Nevada Test Site [abs.]: Geological Society of America Abstracts with Programs, v. 14, no. 6, p. 302.

Bath, G. D., Jahren, C. E., Rosenbaum, J. G., and Baldwin, M. J., 1983, Magnetic investigations, in Geologic and geophysical investigations of Climax stock intrusive, Nevada: U.S. Geological Survey Open-File Report 83-377, p. 40-77.

Boynton, G. R., Meuschke, J. L., and Vargo, J. L., 1963a, Aeromagnetic map of the Timber Mountain quadrangle and part of the Silent Canyon quadrangle, Nye County, Nevada: U.S. Geological Survey Geophysical Investigations Map GP-443, scale 1:62,500.

_____1963b, Aeromagnetic map of the Tippipah Spring quadrangle and parts of the Papoose Lake and Wheelbarrow Peak quadrangles, Nye County, Nevada: U.S. Geological Survey Geophysical Investigations Map GP-441, scale 1:62,500.

Boynton, G. R., and Vargo, J. L., 1963a, Aeromagnetic map of the Cane Spring quadrangle and parts of Frenchman Lake, Specter Range, and Mercury quadrangles, Nye County, Nevada: U.S. Geological Survey Geophysical Investigations Map GP-442, scale 1:62,500.

_____1963b, Aeromagnetic map of the Topopah Spring quadrangle and part of the Bare Mountain quadrangle, Nye County, Nevada: U.S. Geological Survey Geophysical Investigations Map GP-440, scale 1:62,500.

Christiansen, R. L., and Lipman, P. W., 1965, Geologic map of the Topopah Spring NW quadrangle, Nye County, Nevada: U.S. Geological Survey Geologic Quadrangle Map GQ-444, scale 1:24,000.

Dixon, G. L., Quinlivan, W. D., Ray, J. M., and Ohl, J. P., 1975, Supplementary lithologic logs and stratigraphic identifications for exploratory and emplacement drill holes in Areas 3, 4, and 7, Nevada Test Site: U.S. Geological Survey Report USGS 474-211, 87 p.; available only from U.S. Department of Commerce, National Technical Information Service, Springfield, VA 22161.

Douglas, A. C., and Millett, M. R., 1978, Total intensity magnetometer logging as a stratigraphic tool in Tertiary volcanic rock: Lawrence Livermore National Laboratory Report UCRL-52617, p. 1-11.

Fernald, A. T., Corchary, G. S., and Williams, W. P., 1968, Surficial geologic map of Yucca Flat, Nye and Lincoln Counties, Nevada: U.S. Geological Survey Miscellaneous Geologic Investigations Map I-550, scale 1:48,000.

Gordon, Mackenzie, Jr., and Poole, F. G., 1968, Mississippian-Pennsylvanian boundary in southwestern Nevada and southeastern California, in Nevada Test Site: Geological Society of America Memoir 110, p. 157-168.

Henderson, R. G., and Zietz, Isidore, 1949, The upward continuation of anomalies in total magnetic intensity fields: Geophysics, v. 14, no. 4, p. 517-535.

Jahren, C. E., and Bath, G. D., 1967, Rapid estimation of induced and remanent magnetization of rock samples, Nevada Test Site: U.S. Geological Survey Open-File Report, 29 p.

Kane, M. F., and Bracken, R. E., 1983, Aeromagnetic map of Yucca Mountain and surrounding regions, southwest Nevada: U.S. Geological Survey Open-File Report 83-616, 19 p.

Kane, M. F., Webring, M. W., and Bhattacharyya, B. K., 1981, A preliminary analysis of gravity and aeromagnetic surveys of the Timber Mountain area, southern Nevada: U.S. Geological Survey Open-File Report 81-189, 40 p.

Koulomzine, Th., Lamontagne, Y., and Nadeau, A., 1970, New methods for the direct interpretation of magnetic anomalies caused by inclined dikes of infinite length: Geophysics, v. 35, p. 812-830.

Lipman, P. W., and McKay, E. J., 1965, Geologic map of the Topopah Spring SW quadrangle, Nye County, Nevada: U.S. Geological Survey Geologic Quadrangle Map GQ-439, scale 1:24,000.

Maldonado, Florina, and Koether, S. L., 1983, Stratigraphy, structure, and some petrographic features of Tertiary volcanic rocks at the USW G-2 drill hole, Yucca Mountain, Nye County, Nevada: U.S. Geological Survey Open-File Report 83-732, 83 p.

Jung, Karl, 1953, Some remarks on the interpretation of gravity and magnetic anomalies: Geophysical Prospecting, v. 1, p. 29-35.

Philbin, P. W., and White, B. L., Jr., 1965a, Aeromagnetic map of parts of the Cactus Peak and Stinking Spring quadrangles, Nye County, Nevada: U.S. Geological Survey Geophysical Investigations Map GP-517, scale 1:62,500.

_____1965b, Aeromagnetic map of parts of the Kawich Peak and Reveille Peak quadrangles, Nye County, Nevada: U.S. Geological Survey Geophysical Investigations Map GP-516, scale 1:62,500.

Philbin, P. W., 1965c, Aeromagnetic map of the Cactus Spring quadrangle and part of the Goldfield quadrangle, Esmeralda and Nye Counties, Nevada: U.S. Geological Survey Geophysical Investigations Map GP-511, scale 1:62,500.

_____1965d, Aeromagnetic map of the Mellan quadrangle, Nye County, Nevada: U.S. Geological Survey Geophysical Investigations Map GP-518, scale 1:62,500.

_____1965e, Aeromagnetic map of the Quartzite Mountain quadrangle, Nye County, Nevada: U.S. Geological Survey Geophysical Investigations Map GP-515, scale 1:62,500.

_____1965f, Aeromagnetic map of the Belted Peak quadrangle and part of White Blotch Springs quadrangle, Nye County, Nevada: U.S. Geological Survey Geophysical Investigations Map GP-514, scale 1:62,500.

_____1965g, Aeromagnetic map of the Sarcobatus Flat area, Esmeralda and Nye Counties, Nevada: U.S. Geological Survey Geophysical Investigations Map GP-512, scale 1:125,000.

_____1965h, Aeromagnetic map of the Black Mountain quadrangle, Nye County, Nevada: U.S. Geological Survey Geophysical Investigations Map GP-519, scale 1:62,500.

Philbin, P. W., and White, B. L., Jr., 1965i, Aeromagnetic map of the Silent Canyon quadrangle, Nye County, Nevada: U.S. Geological Survey Geophysical Investigations Map GP-520, scale 1:62,500.

_____1965j, Aeromagnetic map of the Wheelbarrow Peak quadrangle and part of the Groom Mine quadrangle, Nye and Lincoln Counties, Nevada: U.S. Geological Survey Geophysical Investigations Map GP-513, scale 1:62,500.

Powell, D. W., 1967, Fitting observed profiles to a magnetized dike or fault-step model: Geophysical Prospecting, v. 15, p. 208-220.

Qureshi, I. R., and Nalaye, A. M., 1978, A method for the direct interpretation of magnetic anomalies caused by two-dimensional vertical faults: Geophysics, v. 43, p. 179-188.

Spengler, R. W., Byers, F. M., Jr., and Warner, J. B., 1981, Stratigraphy and structure of volcanic rocks in drill hole USW-G1, Yucca Mountain, Nye County, Nevada: U.S. Geological Survey Open-File Report 81-1349, 50 p.

U.S. Geological Survey, 1979, Aeromagnetic map of the Timber Mountain area, Nevada: U.S. Geological Survey Open-File Report 79-587, scale 1:62,500.

Vacquier, Victor, Steenland, N. C., Henderson, R. G., and Zietz, Isidore, 1951, Interpretation of aeromagnetic maps: Geological Society of America Memoir 47, 151 p.